

---

---

# AN INTRODUCTION TO OPTICAL FIBERS

---

**Allen H. Cherin**

Bell Laboratories  
Atlanta, Georgia

**Claudio Kitano**  
Dpto. Eng.<sup>a</sup> Elétrica  
FEIS - UNESP

McGRAW-HILL BOOK COMPANY

Auckland Bogotá Guatemala Hamburg Lisbon  
London Madrid Mexico New Delhi Panama Paris  
San Juan São Paulo Singapore Sydney Tokyo

2. The incident field  $\bar{E}_1 = 5e^{-j\beta_1 \theta_1} \hat{a}_x$   
 3.  $\theta_1 = 30^\circ$

I. Find

- a. The magnitude of the field in medium 2 at  $z = 10 \mu\text{m}$   
 b. The  $z$  component of the Poynting vector in medium 2

- II. What is the smallest value of  $\theta_1$  at which total internal reflection will occur?  
**2-5** Refer again to Fig. 2-11. What happens to the wave in medium 2 if  $\theta_1 = 75^\circ$ ? Assume for this case that the wave in medium 2 is given by

$$\bar{E}_T = E_2 e^{-jk_2 z} \hat{a}_z$$

- Find the magnitude of the wave in medium 2 at  $z = 10 \mu\text{m}$  and the  $z$  component of the Poynting vector.

- 2-6** Calculate the group and phase velocities of a wave of free-space wavelength  $\lambda_0 = 1.2 \mu\text{m}$
- (a) in free space,
  - (b) in a nondispersive medium of refractive index 1.4482, and
  - (c) in fused silica (refer to Fig. 5-5 for the  $n(\lambda_0)$  curve of fused silica).

## CHAPTER THREE

### BASIC WAVEGUIDE EQUATIONS, WAVE AND RAY OPTICS

#### 3-1 INTRODUCTION

This chapter is concerned with the development of the basic equations needed for the analysis of dielectric waveguides. Both wave and ray optics models will be developed to analyze the slab waveguide and the round optical fiber.

Since our intent is to design a guiding structure, we will choose the  $z$  axis as the longitudinal axis of our waveguide and assume that energy in the guide is propagating in the  $z$  direction. Our wave optics analysis will use the field theory notation of Chap. 2 to derive a wave equation in terms of the longitudinal components of the fields in the guide. Simple transformation equations will also be derived allowing one to calculate the transverse components of the fields in terms of the longitudinal components.

An alternate ray optics model for analyzing dielectric waveguides will also be developed. The Eikonal equation, which forms the basis of geometric optics, will be derived from the general wave equation. Ray optics equations for inhomogeneous dielectric media will then be transformed in cylindrical coordinates for future use in the analysis of the round optical fiber.

#### 3-2 BASIC WAVEGUIDE EQUATIONS; WAVE OPTICS

Consider the general waveguide structure shown in Fig. 3-1. Our purpose in this section is to develop the mathematical model that will enable us to analyze and design a structure. We will ultimately apply this general model to obtain

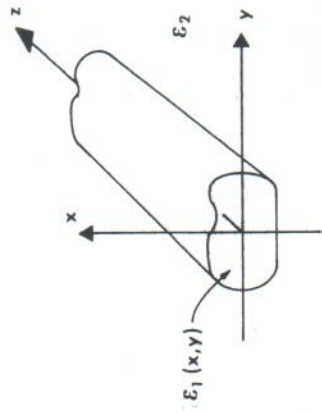


Figure 3-1 General dielectric waveguide structure used to propagate energy in the  $z$  direction.

and

$$\left( \frac{\partial E_z}{\partial y} - \frac{\partial E_y}{\partial z} \right) \hat{a}_x + \left( \frac{\partial E_x}{\partial z} - \frac{\partial E_z}{\partial x} \right) \hat{a}_y + \left( \frac{\partial E_y}{\partial x} - \frac{\partial E_x}{\partial y} \right) \hat{a}_z = -\mu \frac{\partial H_x}{\partial t} \hat{a}_x - \mu \frac{\partial H_y}{\partial t} \hat{a}_y - \mu \frac{\partial H_z}{\partial t} \hat{a}_z \quad (3-4)$$

Since we are assuming that the fields are varying with respect to time as  $e^{j\omega t}$ , we can use Eqs. (3-1) and (3-2) to write the derivatives with respect to  $t$  and  $z$  explicitly as

$$\frac{\partial E_x}{\partial t} = j\omega E_x \quad \frac{\partial E_y}{\partial t} = j\omega E_y \quad \frac{\partial E_z}{\partial t} = j\omega E_z \quad (3-5a)$$

$$\frac{\partial H_x}{\partial t} = j\omega H_x \quad \frac{\partial H_y}{\partial t} = j\omega H_y \quad \frac{\partial H_z}{\partial t} = j\omega H_z \quad (3-5b)$$

$$\frac{\partial E_y}{\partial z} = -j\beta E_y \quad \frac{\partial E_x}{\partial z} = -j\beta E_x \quad (3-5c)$$

$$\frac{\partial H_y}{\partial z} = -j\beta H_y \quad \frac{\partial H_x}{\partial z} = -j\beta H_x \quad (3-5d)$$

Substituting (3-5) into (3-3) and (3-4) and writing in component form we obtain

$$\frac{\partial H_z}{\partial y} + j\beta H_y = j\omega \epsilon E_x \quad (3-6a)$$

$$-j\beta H_x - \frac{\partial H_z}{\partial x} = j\omega \epsilon E_y \quad (3-6b)$$

$$\frac{\partial H_y}{\partial x} - \frac{\partial H_z}{\partial y} = j\omega \epsilon E_z \quad (3-6c)$$

$$\frac{\partial E_z}{\partial y} + j\beta E_y = -j\omega \mu H_x \quad (3-7a)$$

$$-j\beta E_x - \frac{\partial E_z}{\partial x} = -j\omega \mu H_y \quad (3-7b)$$

$$\frac{\partial E_y}{\partial x} - \frac{\partial E_z}{\partial y} = -j\omega \mu H_z \quad (3-7c)$$

We would like to manipulate Eqs. (3-6) and (3-7) to express  $E_x$ ,  $E_y$ ,  $H_x$ ,  $H_y$  in terms of  $E_z$  and  $H_z$  (the transverse components in terms of the longitudinal components).

the “modes” in a dielectric slab waveguide and in a round optical fiber. A mode is an allowable field configuration, for a given waveguide geometry, that satisfies Maxwell’s equations (or the derived wave equations) and all of the boundary conditions of the problem. Our wave optics model will yield a complete description of the fields, that is, expressions for the amplitude and components of the propagation vector of the fields associated with a mode will be obtained.

We will assume that our design objective is to create a dielectric waveguide that propagates energy in a given direction. We define the longitudinal axis of our waveguide as the  $z$  axis and design it such that energy is propagating in the guide in the  $z$  direction with a longitudinal propagation constant  $\beta$ . ( $\beta$  is the longitudinal component of the propagation vector  $\mathbf{k}$ .) We will assume that the permittivity  $\epsilon(x, y)$  does not depend on  $z$  but can vary with  $x$  and  $y$ . This special case of an inhomogeneous medium in which  $\epsilon$  is independent of one space coordinate is an excellent representation of an optical fiber.

Using the notation developed in Chap. 2 and the assumptions cited above, we can write the fields in a waveguide as follows:

$$\bar{E} = \bar{E}_0(x, y)e^{-j\beta z} \quad (3-1)$$

$$\bar{H} = \bar{H}_0(x, y)e^{-j\beta z} \quad (3-2)$$

where the propagation constant  $\beta$  is to be determined.

If we substitute the fields into Maxwell’s equations (2-49) and (2-48) we obtain in expanded component form

$$\begin{aligned} \left( \frac{\partial H_z}{\partial y} - \frac{\partial H_y}{\partial z} \right) \hat{a}_x + \left( \frac{\partial H_x}{\partial z} - \frac{\partial H_z}{\partial x} \right) \hat{a}_y + \left( \frac{\partial H_y}{\partial x} - \frac{\partial H_x}{\partial y} \right) \hat{a}_z \\ = \epsilon \frac{\partial E_x}{\partial t} \hat{a}_x + \epsilon \frac{\partial E_y}{\partial t} \hat{a}_y + \epsilon \frac{\partial E_z}{\partial t} \hat{a}_z \end{aligned} \quad (3-3)$$

Once we accomplish that task our ultimate goal is to derive equations in terms of the longitudinal field components only ( $E_z$  and  $H_z$ ). We will then use these equations to analyze dielectric waveguides.

Working with Eqs. (3-6a) and (3-7b), for example, we can obtain  $E_x$  in terms of  $H_z$  and  $E_z$ . Substituting (3-7b) into (3-6a)

$$j\omega\epsilon E_x = \frac{\partial H_z}{\partial y} + \frac{j\beta}{-\omega\mu} \left( -j\beta E_x - \frac{\partial E_z}{\partial x} \right)$$

or

$$\left( j\omega\epsilon + \frac{-j\beta^2}{\omega\mu} \right) E_x = \frac{\partial H_z}{\partial y} + \frac{\beta}{\omega\mu} \frac{\partial E_z}{\partial x}$$

Multiplying both sides of the above equation by  $-j\omega\mu$

$$(\omega^2\mu\epsilon - \beta^2)E_x = -j \left( \omega\mu \frac{\partial H_z}{\partial y} + \beta \frac{\partial E_z}{\partial x} \right)$$

Let

$$k^2 = k^2 - \beta^2 \quad k^2 = \omega^2\mu\epsilon \quad (3-8)$$

We obtain

$$E_x = \frac{-j}{\kappa^2} \left( \omega\mu \frac{\partial H_z}{\partial y} + \beta \frac{\partial E_z}{\partial x} \right) \quad (3-9)$$

Starting with (3-6b) and (3-7a) in a similar fashion we can obtain

$$E_y = \frac{-j}{\kappa^2} \left( \beta \frac{\partial E_z}{\partial y} - \omega\mu \frac{\partial H_z}{\partial x} \right) \quad (3-10)$$

Using Eqs. (3-7a) and (3-6b) we obtain

$$H_x = \frac{-j}{\kappa^2} \left( \beta \frac{\partial H_z}{\partial x} - \omega\epsilon \frac{\partial E_z}{\partial y} \right) \quad (3-11)$$

and using (3-7b) and (3-6a) we obtain

$$H_y = \frac{-j}{\kappa^2} \left( \beta \frac{\partial H_z}{\partial y} + \omega\epsilon \frac{\partial E_z}{\partial x} \right) \quad (3-12)$$

If we could solve for the longitudinal components of the fields we can, using Eqs. (3-9) to (3-12), obtain the transverse components.

We are now interested in deriving equations in terms of the longitudinal field components only ( $E_z$  and  $H_z$ ).

If in Eq. (3-6c) we substitute (3-11) and (3-12) we obtain

$$\frac{-j}{\kappa^2} \beta \frac{\partial^2 H_z}{\partial x \partial y} - \frac{j}{\kappa^2} \omega\epsilon \frac{\partial^2 E_z}{\partial x^2} + \frac{j}{\kappa^2} \beta \frac{\partial^2 H_z}{\partial y^2} - \frac{j}{\kappa^2} \omega\epsilon \frac{\partial^2 E_z}{\partial y^2} = j\omega\epsilon E_z$$

multiplying by  $j\kappa^2/\omega\epsilon$  we obtain

$$\frac{\partial^2 E_z}{\partial x^2} + \frac{\partial^2 E_z}{\partial y^2} + \kappa^2 E_z = 0 \quad (3-13)$$

This is a partial differential equation in  $E_z$  only. In a similar manner, starting with Eq. (3-7c) and substituting Eqs. (3-9) and (3-10) we can derive

$$\frac{\partial^2 H_z}{\partial x^2} + \frac{\partial^2 H_z}{\partial y^2} + \kappa^2 H_z = 0 \quad (3-14)$$

Equations (3-13) and (3-14) are modified forms of a wave equation and can be rewritten as follows:

$$\nabla_T^2 E_z + \kappa^2 E_z = 0 \quad (3-15)$$

$$\nabla_T^2 H_z + \kappa^2 H_z = 0 \quad (3-16)$$

where

$$\nabla_T^2 = \frac{\partial^2}{\partial x^2} + \frac{\partial^2}{\partial y^2} \quad (3-17)$$

$\nabla_T^2$  is the transverse laplacian operator.

We will use Eqs. (3-15) and (3-16) transformed into cylindrical coordinates to derive the fields in a round optical fiber. In general when  $\epsilon$  depends on  $x$  and  $y$ , (3-15) and (3-16) are no longer exact, since derivatives with respect to  $x$  and  $y$  of  $\epsilon$  were not taken. ( $\epsilon$  was assumed to be a constant.) However, they are still good approximations if the variation in  $\epsilon$  is small over the region of one wavelength. For the graded index optical fiber this approximation is a very good one.

It is interesting to note that Eqs. (3-15) and (3-16) are uncoupled equations in the longitudinal component of the fields only. In general coupling of the two longitudinal fields occurs when satisfying the boundary conditions of a problem. This is the case for the round optical fiber. If the boundary conditions do not

Table 3-1 Listing of the various types of modes

Nomenclature	Longitudinal components	Transverse components
TEM (transverse electromagnetic)	$E_z = 0$ $H_z = 0$	$E_T, H_T$
TE (transverse electric)	$E_z = 0$ $H_z \neq 0$	$E_T, H_T$
TM (transverse magnetic)	$H_z = 0$ $E_z \neq 0$	$E_T, H_T$
HE or EH (hybrid)	$H_z \neq 0$ $E_z \neq 0$	$E_T, H_T$

achieve coupling of the longitudinal components, it is possible to obtain mode solutions with either  $E_z = 0$  (transverse electric (TE) mode) or  $H_z = 0$  (transverse magnetic (TM) mode). A list of the different types of modal solutions that can exist in an infinite dielectric medium or in a dielectric waveguide are given in Table 3-1.

**Example 3-1 Transverse components of a TM mode** Using Eqs. (3-9) to (3-12) we can illustrate how to calculate the transverse field components of a TM mode in a waveguide in terms of the longitudinal field components.

For a TM mode,  $H_z = 0$ . The transverse field components are given by Eqs. (3-9) to (3-12) with  $H_z = 0$ .

$$E_x = \frac{-j}{\kappa^2} \beta \frac{\partial E_z}{\partial x}$$

$$E_y = \frac{-j}{\kappa^2} \beta \frac{\partial E_z}{\partial y}$$

$$H_x = \frac{j}{\kappa^2} \omega \epsilon \frac{\partial E_z}{\partial y}$$

$$H_y = \frac{-j}{\kappa^2} \omega \epsilon \frac{\partial E_z}{\partial x}$$

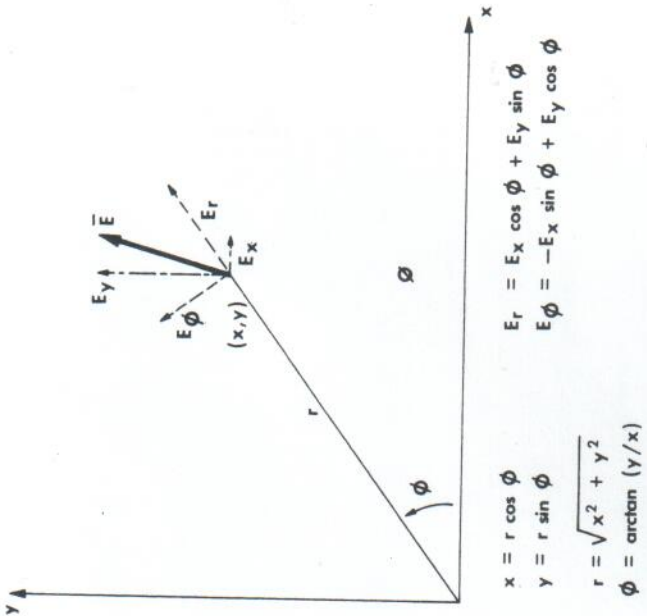


Figure 3-2 Geometry for conversion from cartesian to cylindrical coordinates.

### 3-3 WAVEGUIDE EQUATIONS IN CYLINDRICAL COORDINATES

In Sec. 3-2 we developed a mathematical model for analyzing dielectric waveguides with their fields propagating in the z direction. This model consisted of a set of equations ((3-9) to (3-12)) relating the transverse components to the longitudinal components of the fields, and two modified wave equations (3-15) and (3-16) written in terms of the longitudinal components of the fields of the waveguide only. Now we will convert the above equations from cartesian coordinates to cylindrical coordinates so that we may apply them in Chap. 5 to the geometry of the round optical fiber. The geometry considered in converting from cartesian coordinates to cylindrical coordinates is shown in Fig. 3-2. The z coordinate, which is the optical axis of our system, is common to both coordinate systems. As an example of the coordinate conversion process consider expressing  $E_r$  in cylindrical coordinates

$$E_r = E_x \cos \phi + E_y \sin \phi \quad (3-18)$$

where in cartesian coordinates  $E_x$  and  $E_y$  are given by Eqs. (3-9) and (3-10).

$$\begin{aligned} x &= r \cos \phi & E_r &= E_x \cos \phi + E_y \sin \phi \\ y &= r \sin \phi & E_\phi &= -E_x \sin \phi + E_y \cos \phi \\ r &= \sqrt{x^2 + y^2} \\ \phi &= \arctan(y/x) \end{aligned} \quad (3-21)$$

Substituting these equations into (3-18)

$$E_r = \frac{-j}{\kappa^2} \left( \omega \mu \frac{\partial H_z}{\partial y} \cos \phi + \beta \frac{\partial E_z}{\partial x} \cos \phi + \beta \frac{\partial E_z}{\partial y} \sin \phi - \omega \mu \frac{\partial H_z}{\partial x} \sin \phi \right) \quad (3-19)$$

Using the chain rule to obtain the required partial derivatives in cylindrical coordinates

$$\begin{aligned} \frac{\partial f}{\partial x} &= \frac{\partial f}{\partial r} \frac{\partial r}{\partial x} + \frac{\partial f}{\partial \phi} \frac{\partial \phi}{\partial x} \\ \frac{\partial f}{\partial y} &= \frac{\partial f}{\partial r} \frac{\partial r}{\partial y} + \frac{\partial f}{\partial \phi} \frac{\partial \phi}{\partial y} \end{aligned}$$

where

$$\frac{dr}{dx} = \frac{x}{r} = \cos \phi \quad \frac{d\phi}{dx} = \frac{-y}{r^2} = \frac{-\sin \phi}{r} \quad (3-18)$$

$$\begin{aligned} \frac{dr}{dy} &= \frac{y}{r} = \sin \phi & \frac{d\phi}{dy} &= \frac{x}{r^2} = \frac{\cos \phi}{r} \end{aligned} \quad (3-21)$$

equations or the wave equation. Ray optics can be applied to all phenomena that are described by the wave equation and that satisfy the additional requirement that the wavelength of light is short compared to the dimensions of the guide through which it passes. For example, ray optics can be used in a large-core multimode optical fiber. Ray optics is also useful because it allows one to visualize propagation of light rays in a simple way. One can think of ray optics as being very similar to the classical mechanics of a point particle.<sup>2</sup> In fact the relation between wave and ray optics is analogous to the relation between wave mechanics and ordinary mechanics of a point particle.

In this section the relationship between wave and ray optics will be shown by deriving the equations of ray optics from the wave equation developed in Chap. 2. If you will recall the Helmholtz equation (2-52)

Simplifying Eq. (3-22) yields

$$E_r = \frac{-j}{\kappa^2} \left( \beta \frac{\partial E_z}{\partial r} + \omega \mu \frac{1}{r} \frac{\partial H_z}{\partial \phi} \right) \quad (3-23)$$

Following the same procedures the equations for  $E_\phi$ ,  $H_r$ ,  $H_\phi$  can be written in cylindrical coordinates in terms of  $E_z$  and  $H_z$  as

$$E_\phi = \frac{-j}{\kappa^2} \left( \beta \frac{1}{r} \frac{\partial E_z}{\partial \phi} - \omega \mu \frac{\partial H_z}{\partial r} \right) \quad (3-24)$$

$$H_r = \frac{-j}{\kappa^2} \left( \beta \frac{\partial H_z}{\partial r} - \omega \epsilon \frac{1}{r} \frac{\partial E_z}{\partial \phi} \right) \quad (3-25)$$

$$H_\phi = \frac{-j}{\kappa^2} \left( \beta \frac{1}{r} \frac{\partial H_z}{\partial \phi} + \omega \epsilon \frac{\partial E_z}{\partial r} \right) \quad (3-26)$$

In addition the modified wave equations (3-15) and (3-16) in cylindrical coordinates become

$$\frac{\partial^2 E_z}{\partial r^2} + \frac{1}{r} \frac{\partial E_z}{\partial r} + \frac{1}{r^2} \frac{\partial^2 E_z}{\partial \phi^2} + \kappa^2 E_z = 0 \quad (3-27)$$

and

$$\frac{\partial^2 H_z}{\partial r^2} + \frac{1}{r} \frac{\partial H_z}{\partial r} + \frac{1}{r^2} \frac{\partial^2 H_z}{\partial \phi^2} + \kappa^2 H_z = 0 \quad (3-28)$$

Equations (3-27) and (3-28) will be solved in Chap. 5 to obtain expressions for  $E_z$  and  $H_z$  in a round optical fiber. These expressions will then be substituted into (3-23) to (3-26) to obtain a complete description of the fields in a fiber.

#### 3-4 RAY OPTICS; THE EIKONAL AND RAY EQUATIONS

An alternate method of analyzing optical waveguides is through the use of a geometric or ray optics model. Ray optics allows us to treat light propagation in a way that is far simpler than would be possible by solving Maxwell's

equations or the wave equation. Ray optics can be applied to all phenomena that are described by the wave equation and that satisfy the additional requirement that the wavelength of light is short compared to the dimensions of the guide through which it passes. For example, ray optics can be used in a large-core multimode optical fiber. Ray optics is also useful because it allows one to visualize propagation of light rays in a simple way. One can think of ray optics as being very similar to the classical mechanics of a point particle.<sup>2</sup> In fact the relation between wave and ray optics is analogous to the relation between wave mechanics and ordinary mechanics of a point particle.

In this section the relationship between wave and ray optics will be shown by deriving the equations of ray optics from the wave equation developed in Chap. 2. If you will recall the Helmholtz equation (2-52)

$$\nabla^2 \bar{E} + k^2 \bar{E} = 0 \quad (3-29)$$

and if  $\psi$  is any rectangular component of  $\bar{E}$

$$\nabla^2 \psi + k^2 \psi = 0 \quad (3-30)$$

where

$$k = nk_0 = n \left( \frac{2\pi}{\lambda_0} \right) \quad (3-31)$$

We will seek a solution to Eq. (3-30) of the form

$$\psi = \psi_0(x, y, z) e^{-jk_0 S(x, y, z)} \quad (3-32)$$

Where  $\psi_0(x, y, z)$  and  $S(x, y, z)$  are real functions of position.  $S(x, y, z)$  is a phase function associated with the medium and is called an "eikonal."

Substituting Eq. (3-32) into (3-30), we obtain

$$\nabla^2(\psi_0 e^{-jk_0 S}) + k^2 \psi_0 e^{-jk_0 S} = 0 \quad (3-33)$$

Note that the laplacian of the product of the two scalar functions in the first term of Eq. (3-33) is

$$\nabla^2(\psi_0 e^{-jk_0 S}) = \psi_0 \nabla^2 e^{-jk_0 S} + e^{-jk_0 S} \nabla^2 \psi_0 + 2\nabla \psi_0 \cdot \nabla e^{-jk_0 S}$$

and

$$\begin{aligned} \nabla^2 e^{-jk_0 S} &= \nabla \cdot \nabla e^{-jk_0 S} = \nabla \cdot [-jk_0 (\nabla S) e^{-jk_0 S}] \\ &= [-k_0^2 (\nabla S)^2 - jk_0 \nabla^2 S] e^{-jk_0 S} \end{aligned}$$

where

$$(\nabla S)^2 = \nabla S \cdot \nabla S = \left( \frac{\partial S}{\partial x} \right)^2 + \left( \frac{\partial S}{\partial y} \right)^2 + \left( \frac{\partial S}{\partial z} \right)^2$$

Therefore

$$\begin{aligned} \nabla^2(\psi_0 e^{-jk_0 S}) &= \psi_0 [ -k_0^2 (\nabla S)^2 - jk_0 \nabla^2 S ] e^{-jk_0 S} \\ &\quad + e^{-jk_0 S} \nabla^2 \psi_0 - j2k_0 e^{-jk_0 S} \nabla S \cdot \nabla \psi_0 \end{aligned} \quad (3-34)$$

Substituting Eq. (3-34) into (3-33) and dividing out the common  $e^{-jk_0 S}$  term results in

$$\psi_0 [-k_0^2(\nabla S)^2 - jk_0 \nabla^2 S] + \nabla^2 \psi_0 - jk_0 \nabla S \cdot \nabla \psi_0 + k^2 \psi_0 = 0 \quad (3-35)$$

Finally equating the real and imaginary parts of Eq. (3-35) we obtain real part

$$-\psi_0 k_0^2 (\nabla S)^2 + \nabla^2 \psi_0 + k^2 \psi_0 = 0 \quad (3-36a)$$

and imaginary part

$$\psi_0 \nabla^2 S + 2VS \cdot \nabla \psi_0 = 0 \quad (3-36b)$$

Equations (3-36a) and (3-36b) represent an exact solution to the original wave equation (3-30). To obtain the simplifying geometric optics approximation to Eq. (3-36a) we will rewrite it in convenient form and show that one of the terms may be neglected as  $\lambda_0$  becomes very small.

Rearranging Eq. (3-36a)

$$(\nabla S)^2 - \frac{\nabla^2 \psi_0}{k_0^2 \psi_0} = n^2 \quad (3-37)$$

notice that  $k_0 = 2\pi/\lambda_0$  and

$$\frac{\nabla^2 \psi_0}{k_0^2 \psi_0} = \frac{\lambda_0^2 (\nabla^2 \psi_0)}{(2\pi)^2 \psi_0} \quad (3-38)$$

As  $\lambda_0$  becomes very small, that is, as  $\lambda_0$  approaches zero, Eq. (3-38) approaches zero and Eq. (3-37) becomes

$$(\nabla S)^2 = n^2 \quad (3-39)$$

Equation (3-39) is known as the "eikonal" equation. It determines the function  $S$ , which allows us to define the surfaces of constant phase by the equation

$$S(x, y, z) = \text{const} \quad (3-40)$$

These surfaces of constant phase define the shape of the fields. The eikonal equation determines, within the geometrical optics approximation, the wave propagation in a guide.

We know from Chap. 2 that the surfaces of constant phase are perpendicular to the direction of light propagation of a plane wave. We will now define light rays as the locus of points that form the orthogonal trajectories to the constant phase fronts of a light wave. If we know the surfaces of constant phase, we can construct the light rays by drawing lines perpendicular to the phase fronts. As the phase fronts curve in an inhomogeneous medium, so do the light rays.

It is often desirable to calculate the trajectories of the light rays directly without having to construct the phase fronts from the eikonal equation. In order to develop the equations for the trajectories of light rays consider the

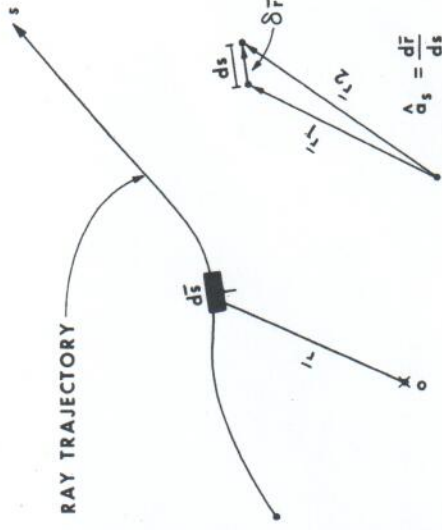


Figure 3-3 Geometry for ray trajectory equations.

geometry of a ray path shown in Fig. 3-3. A radius vector  $\bar{r}$  is drawn from a fixed origin  $O$  to an arbitrary point on a ray path. If this vector  $\bar{r}$  were known for all points along the ray, we would have a mathematical description of the light ray. Our strategy will be to develop an equation in terms of the radius vector  $\bar{r}$ , the distance measured along the ray  $s$ , and the refractive index of the medium  $n$ .

From the eikonal equation we have information about a vector  $\nabla S$  that is perpendicular to the phase fronts in the direction of a ray. That is

$$\nabla S = n \hat{a}_s \quad (3-41)$$

where  $\hat{a}_s$  is a unit vector tangent to the light ray. From Fig. 3-3 it is evident that

$$\hat{a}_s = \frac{d\bar{r}}{ds} \quad (3-42)$$

$$\nabla S = n \frac{d\bar{r}}{ds} \quad (3-43)$$

We wish now to incorporate the information in Eq. (3-43) into the eikonal equation so that we can eliminate  $S$  and obtain an equation in terms of  $\bar{r}$ ,  $s$ , and  $n$ . To accomplish this first observe that

$$\frac{d}{ds} \frac{d\bar{r}}{ds} \cdot \nabla = \frac{d}{ds} (x\hat{a}_x + y\hat{a}_y + z\hat{a}_z) \cdot \left( \frac{\partial}{\partial x} \hat{a}_x + \frac{\partial}{\partial y} \hat{a}_y + \frac{\partial}{\partial z} \hat{a}_z \right) \quad (3-44)$$

Using (3-44)

$$\frac{d}{ds} (\nabla S) = \hat{a}_s \cdot \nabla (\nabla S) = \hat{a}_s \cdot (\nabla \nabla S) \quad (3-45)$$

where  $\nabla V$  is the dyadic tensor operator. We can obtain an expression for  $\nabla V$  if we take the gradient of the eikonal equation (3-39)

$$\nabla S \cdot \nabla \nabla S = n \nabla n \quad (3-46)$$

Now from Eqs. (3-41) and (3-46) we obtain

$$\hat{a}_s \cdot (\nabla \nabla S) = \frac{\nabla S}{n} \cdot \nabla \nabla S = \nabla n \quad (3-47)$$

Using Eq. (3-45) yields

$$\frac{d}{ds} (\nabla S) = \nabla n \quad (3-48)$$

or using Eq. (3-43) we obtain the desired ray trajectory equation

$$\frac{d}{ds} \left( n \frac{d\vec{r}}{ds} \right) = \nabla n \quad (3-49)$$

All of ray optics can be derived from the ray equation (3-49). The ray equation describes the trajectory of a light beam by the position vector  $\vec{r} = \vec{r}(s)$ , which is a function of the length of the ray measured from some arbitrary starting point. The ray equation contains the refractive index,  $n(x, y, z)$ , as well as the gradient of the refractive index  $\nabla n(x, y, z)$ . As shown in Example 3-2 when the medium is homogeneous the rays will be straight lines. When the medium is inhomogeneous ( $\nabla n \neq 0$ ) the ray trajectories will be curved paths.

The ray equation is expressed in vector form in Eq. (3-49) and is independent of the choice of the coordinate system it is expressed in. In cartesian coordinates, the component equations of the ray equation are

$$\frac{d}{ds} \left( n \frac{dx}{ds} \right) = \frac{\partial n}{\partial x} \quad (3-50)$$

$$\frac{d}{ds} \left( n \frac{dy}{ds} \right) = \frac{\partial n}{\partial y} \quad (3-51)$$

$$\frac{d}{ds} \left( n \frac{dz}{ds} \right) = \frac{\partial n}{\partial z} \quad (3-52)$$

One of the most important theorems of ray optics (Snell's law) can be derived from Eq. (3-52). If we consider three dielectric media as shown in Fig. 3-4 and assume that the refractive indices of these media are a function of  $x$  only, then Eq. (3-52) becomes

$$\frac{d}{ds} \left( n \frac{dz}{ds} \right) = 0 \quad (3-53)$$

since  $\partial n / \partial z = 0$ .

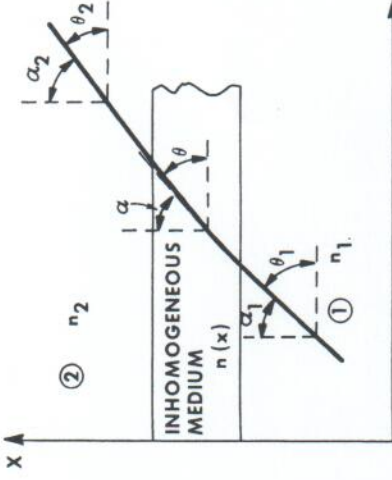


Figure 3-4 Geometry for light-ray development of Snell's law.

$$\hat{a}_s \cdot (\nabla S) = \frac{\nabla S}{n} \cdot \nabla \nabla S = \nabla n \quad (3-54)$$

Integrating Eq. (3-53) we obtain

$$n \frac{dz}{ds} = \text{const} \quad (3-55)$$

From the geometry shown in Fig. 3-4,  $dz/ds$  can be written as follows:

$$\frac{dz}{ds} = \sin \alpha = \cos \theta \quad (3-55)$$

Using Eq. (3-55), Eq. (3-54) becomes

$$n \frac{dz}{ds} = n \cos \theta = n \sin \alpha = \text{const} \quad (3-56)$$

Equation (3-56) is Snell's law derived from a ray optics point of view. Snell's law illustrates the fact that  $n \cos \theta$  is constant along a ray trajectory provided that the refractive index of the media does not depend upon  $z$ . The form of Snell's law that was derived in Chap. 2 (Eq. (2-116)) can be obtained from Eq. (3-56) if we consider media 1 and 2 in Fig. 3-4. Equation (3-56) applied in the regions of constant refractive index  $n_1$  and  $n_2$  becomes

$$n_1 \cos \theta_1 = n_2 \cos \theta_2 \quad (3-57)$$

or, by using the complement of the angles,

$$n_1 \sin \alpha_1 = n_2 \sin \alpha_2 \quad (3-58)$$

Equations (3-57) and (3-58) hold regardless of the shape of the index profile in the transition region and contain only  $n_1$  and  $n_2$ , the refractive indices in the two homogeneous half-space regions.

### 3.5 RAY EQUATION IN CYLINDRICAL COORDINATES

For applications involving optical fibers, we need to know the ray equation in cylindrical coordinates. We will assume once again that the refractive index is independent of  $z$  (longitudinal coordinate) but can be a function of the transverse coordinates  $r$  and  $\phi$ . That is,  $n = n(r, \phi)$ . The transformation from cartesian to cylindrical coordinates of Eqs. (3-50) and (3-51) require the following sets of equations:

$$x = r \cos \phi \quad (3-60a)$$

$$y = r \sin \phi \quad (3-60b)$$

$$r = (x^2 + y^2)^{1/2} \quad (3-61a)$$

$$\phi = \arctan(y/x) \quad (3-61b)$$

The partial derivatives of  $n$  with respect to  $x$  and  $y$  may be expressed as

$$\frac{\partial n}{\partial x} = \frac{\partial n}{\partial r} \frac{\partial r}{\partial x} + \frac{\partial n}{\partial \phi} \frac{\partial \phi}{\partial x} = \frac{\partial n}{\partial r} \cos \phi - \frac{\partial n}{\partial \phi} \frac{\sin \phi}{r} \quad (3-62)$$

$$\frac{\partial n}{\partial y} = \frac{\partial n}{\partial r} \frac{\partial r}{\partial y} + \frac{\partial n}{\partial \phi} \frac{\partial \phi}{\partial y} = \frac{\partial n}{\partial r} \sin \phi + \frac{\partial n}{\partial \phi} \frac{\cos \phi}{r} \quad (3-63)$$

and the derivatives of  $x$  and  $y$  with respect to  $s$  become

$$\frac{dx}{ds} = \frac{\partial r}{\partial s} \cos \phi - r \frac{\partial \phi}{\partial s} \sin \phi \quad (3-64)$$

$$\frac{dy}{ds} = \frac{\partial r}{\partial s} \sin \phi + r \frac{\partial \phi}{\partial s} \cos \phi \quad (3-65)$$

Using Eqs. (3-61) to (3-65) the ray equation can be derived in cylindrical coordinates.<sup>4</sup> Example 3-3 illustrates the derivation of the  $r$  component of the ray equation. Listed below are the components  $r$ ,  $\phi$ , and  $z$  in cylindrical coordinates of the ray equation.

$$\frac{d}{ds} \left( n \frac{dr}{ds} \right) - nr \left( \frac{d\phi}{ds} \right)^2 = \frac{\partial n}{\partial r} \quad (r \text{ component}) \quad (3-66)$$

$$\frac{d}{ds} \left( nr^2 \frac{d\phi}{ds} \right) = \frac{\partial n}{\partial \phi} \quad (\phi \text{ component}) \quad (3-67)$$

$$\frac{d}{ds} \left( n \frac{dz}{ds} \right) = \frac{\partial n}{\partial z} \quad (z \text{ component}) \quad (3-68)$$

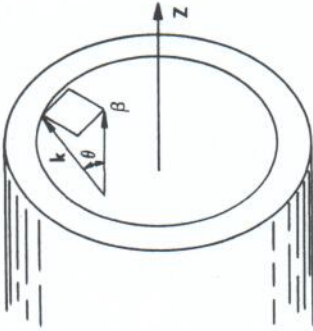


Figure 3-5 Components of propagation vector; ray optics.

$$\cos \theta = \frac{\beta}{k}$$

For a waveguide of the type shown in Fig. 3-1, Eq. (3-53) can be written in terms of  $\beta$  and  $k$ , that is,

$$n \frac{dz}{ds} = n \cos \theta = \text{const} = n \frac{\beta}{k} \quad (3-59)$$

where  $k$  is the magnitude and  $\beta$  the  $z$  component of the propagation vector of the plane wave defining the ray. As shown in Fig. 3-5,  $\theta$  is now the ray angle relative to the  $z$  axis. This physical interpretation of Snell's law will be useful to us when we analyze the round optical fiber in Chaps. 5 and 6.

**Example 3-2 Ray propagation in homogeneous media** Using the ray equation (3-49) it is easy to show that in homogeneous media light rays are straight lines. For a homogeneous medium, the refractive index is a constant and  $\nabla n = 0$ . Therefore the solution of the ray equation (3-49) is immediately obtained as

$$\frac{d\bar{r}}{ds} = \bar{a} = \text{const}$$

Integrating we obtain

$$\bar{r} = \bar{a}s + \bar{b}$$

The above equation for  $\bar{r}$  is the equation of a straight line.

Equations (3-66) to (3-68) are valid even if  $n(r, \phi, z)$ . If  $n$  is independent of  $z$ , Eq. (3-68) becomes Eq. (3-59). If, as is often the case for optical fibers,  $n$  is independent of  $\phi$ , then Eq. (3-67) becomes

$$nr^2 \frac{d\phi}{ds} = \text{const} \quad (3-69)$$

In addition, it is often convenient to approximate the ray equation by replacing  $ds$  with  $dz$ . This approximation is valid if the angle of the ray relative to the  $z$  axis remains small. This approximate form of the ray equation is called the paraxial ray equation since all the rays are nearly parallel to the  $z$  axis. The paraxial approximation also requires that  $n(x, y)$  or  $n(r, \phi)$  varies only a small amount. This allows us to replace  $n(x, y)$  with an average value  $n(x, y) = n_a$ . We will, however, retain the derivative term of  $n$ , since these terms will provide the information about the refracting properties of rays in a medium with a graded index.

The paraxial form of the ray equation (3-49) is

$$\frac{d^2\bar{r}}{dz^2} - r \left( \frac{d\phi}{dz} \right)^2 = \frac{1}{n_a} \nabla n \quad (3-70)$$

and finally the paraxial ray equations in cylindrical coordinates are

$$\frac{d^2r}{dz^2} - r \left( \frac{d\phi}{dz} \right)^2 = \frac{1}{n_a} \frac{\partial n}{\partial r} \quad (3-71)$$

$$\frac{d}{dz} \left( r^2 \frac{d\phi}{dz} \right) = \frac{1}{n_a} \frac{\partial n}{\partial \phi} \quad (3-72)$$

Equations (3-71) and (3-72) will be used in Chap. 6 to analyze the ray trajectories of a graded-index fiber with a parabolic-shaped refractive index profile.

**Example 3-3 Derivation of the radial component of the ray equation** To derive the radial component of the ray equation, we will start with Eqs. (3-50) and (3-51). If we multiply Eq. (3-50) by  $x$  and Eq. (3-51) by  $y$  and add the resulting equations we obtain

$$x \frac{d}{ds} \left( n \frac{dx}{ds} \right) + y \frac{d}{ds} \left( n \frac{dy}{ds} \right) = x \frac{\partial n}{\partial x} + y \frac{\partial n}{\partial y}$$

If we then use Eqs. (3-62) and (3-63) along with Eqs. (3-60a,b) in the above equation we obtain

$$\cos \phi \frac{d}{ds} \left( n \frac{dx}{ds} \right) + \sin \phi \frac{d}{ds} \left( n \frac{dy}{ds} \right) = \frac{\partial n}{\partial r}$$

## REFERENCES

1. D. Marcuse: *Light Transmission Optics*, Van Nostrand Reinhold Co., New York, 1972.
2. J. A. Arnaud: *Beam and Fiber Optics*, Academic Press, New York, 1976.
3. M. Born, and E. Wolf: *Principles of Optics*, Pergamon Press, London, 1970.
4. D. Marcuse: *Principles of Optical Fiber Measurement*, Academic Press, New York, 1981.

## PROBLEMS

3-1 Starting with Eq. (3-7c), derive the modified wave equation in terms of  $H_z$  (Eq. (3-14)).

3-2 For a dielectric waveguide, define the transverse field components of a TE mode in terms of  $H_z$  (longitudinal field component). Which of these field components exist if the field is uniform in the  $y$  direction (i.e.,  $\partial/\partial y = 0$ )?

3-3 Starting with Eq. (3-15), derive the modified wave equation for  $E_z$  in cylindrical coordinates (Eq. (3-27)).

$$\left( \text{In cylindrical coordinates } \nabla_T^2 = \frac{1}{r} \frac{\partial}{\partial r} + r \frac{\partial}{\partial \theta} + \frac{1}{r^2} \frac{\partial^2}{\partial \theta^2} \right)$$

and a source wavelength of  $0.82 \mu\text{m}$ . Specify  $n_1$ ,  $n_2$ , and  $d$  for the guide. Use a diagram similar to Fig. 4-2 to find  $\kappa$  and  $\gamma$  for the TE modes in the guide.

$$n_2 = 1.46$$

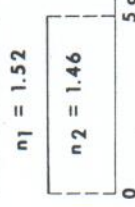


Figure 4-11 Geometry and values of refractive indices of dielectric slab waveguide, Prob. 4-5.

4-5 Estimate the multimode group delay of the dielectric slab waveguide shown in Fig. 4-11 if the length of the guide is 5 cm. Assume that the dispersive properties of the core and cladding glasses are similar.

### 5-1 INTRODUCTION

In this chapter the step-index optical fiber is treated as a boundary-value problem and expressions for the modes in the fiber are obtained. Mode cutoff conditions are then analyzed and a design equation for a single-mode fiber is developed. Next, linearly polarized (LP) modes are introduced along with the concept of a principle mode number to simplify our understanding and analysis of a fiber. Using this simplified notation, expressions that describe the power and delay distortion characteristics in a multimode step-index fiber are derived. Finally a discussion of delay distortion in both single- and multimode fibers is included in this chapter to provide the reader with an understanding of the mechanisms that limit the bandwidth of a step-index fiber.

### 5-2 BASIC EQUATIONS AND PHYSICAL CONSTRAINTS; THE STEP-INDEX FIBER

In the last chapter we developed the concept of propagating modes in a dielectric waveguide by using electromagnetic field theory to rigorously solve the boundary-value problem of the homogeneous slab waveguide. Solutions to a wave equation were found in the core and cladding of the guide and these solutions were matched via the boundary conditions at the core-cladding interface to yield the "characteristic" equations of the guide. Solution of the characteristic equations produced a finite set of propagation constants and their

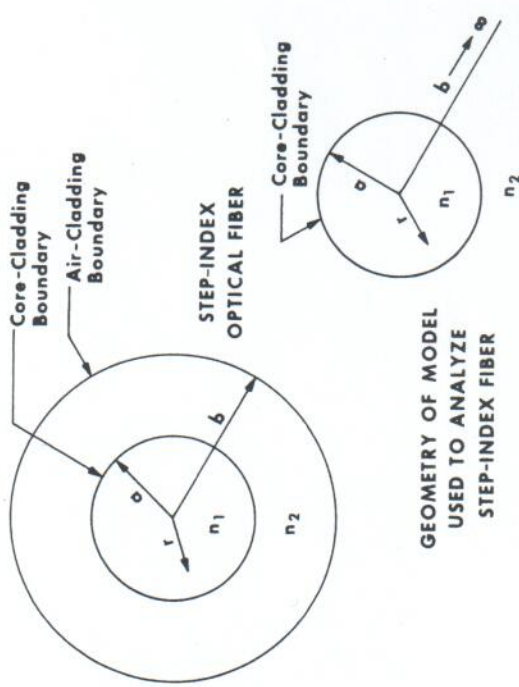


Figure 5-1 Geometry of the step-index fiber and model used for analysis.

associated modes that exist in the guide. To analyze the round optical fiber with a homogeneous core (the step-index fiber) the same general approach that was used for the dielectric slab waveguide will be followed.

First we will assume that  $b$ , the radius of the fiber cladding, is large enough to ensure that the cladding field decays exponentially and approaches zero at the cladding-air interface. This will allow us, as shown in Fig. 5-1, to analyze the fiber as a two-media boundary-value problem. This assumption agrees well with the condition that exists within a properly designed optical fiber. The steps we will follow to solve the boundary-value problem of the step-index fiber are outlined in Table 5-1.

In Sec. 3-3 a set of equations were developed in cylindrical coordinates relating the transverse components to the longitudinal components of the fields for an optical system with cylindrical symmetry. That is a system with fields

propagating in the  $z$  direction. To obtain the modes in a step-index optical fiber, one must solve the modified wave equations (5-1) and (5-2) shown below for  $E_z$  and  $H_z$  in both the core and cladding regions of the fiber. Having obtained expressions for  $E_z$  and  $H_z$  we can directly obtain expressions for the transverse components of the fields  $E_r$ ,  $E_\phi$ ,  $H_r$ , and  $H_\phi$  from Eqs. (3-23) to (3-26).

$$\frac{\partial^2 E_z}{\partial r^2} + \frac{1}{r} \frac{\partial E_z}{\partial r} + \frac{1}{r^2} \frac{\partial^2 E_z}{\partial \phi^2} + \kappa^2 E_z = 0 \quad (5-1)$$

$$\frac{\partial^2 H_z}{\partial r^2} + \frac{1}{r} \frac{\partial H_z}{\partial r} + \frac{1}{r^2} \frac{\partial^2 H_z}{\partial \phi^2} + \kappa^2 H_z = 0 \quad (5-2)$$

Since Eqs. (5-1) and (5-2) have the same mathematical form we will solve (5-1) understanding that solutions obtained for it will be valid for Eq. (5-2). To obtain Eq. (5-1) we have already assumed an optical system with cylindrical symmetry. The longitudinal direction of propagation is the  $z$  axis and the  $z$  and time dependence of the fields is of the form  $e^{j(\omega t - \beta z)}$ .

The technique of separation of variables will now be applied to obtain a solution of Eq. (5-1). We will assume that we can obtain independent solutions for  $E_z$  in  $\phi$  and  $r$ , that is,

$$E_z(\phi, r) = A\Phi(\phi)F(r) \quad (5-3)$$

Since the fiber has circular symmetry we will choose a circular function as a trial solution for  $\Phi(\phi)$ .

$$\Phi(\phi) = e^{jv\phi} \quad (5-4)$$

where  $v$  is a positive or negative integer, and

$$E_z = A F(r) e^{jv\phi} \quad (5-5)$$

Taking the derivatives with respect to  $r$  and  $\phi$  for substitution into Eq. (5-1) we obtain

$$\frac{\partial E_z}{\partial r} = A e^{jv\phi} \frac{dF(r)}{dr} \quad (5-6)$$

$$\frac{\partial^2 E_z}{\partial r^2} = A e^{jv\phi} \frac{d^2 F(r)}{dr^2} \quad (5-7)$$

and

$$\frac{\partial^2 E_z}{\partial \phi^2} = -A v^2 e^{jv\phi} F(r) \quad (5-8)$$

substituting Eqs. (5-6) to (5-8) into (5-1) and multiplying the resulting equation by  $1/A e^{jv\phi}$  one obtains

$$\frac{d^2 F(r)}{dr^2} + \frac{1}{r} \frac{dF(r)}{dr} + \left( \kappa^2 - \frac{v^2}{r^2} \right) F(r) = 0 \quad (5-9)$$

#### Table 5-1 Analysis of step-index fiber—Procedures followed

1. Mathematically model the step-index fiber using the wave equations in cylindrical coordinates.
2. Use the technique of separation of variables to partition the wave equations.
3. Define the physical requirements that influence the solutions of the fields in the core and cladding.
4. Select the proper functional form of the solution of the modified wave equation (Bessel's equation) in the core and cladding.
5. Apply the boundary conditions at the core-cladding interface.
6. Obtain the "characteristic" equation and its resulting modal solutions.
7. Analyze the resulting modes and their cutoff conditions.

Equation (5-9) is a form of Bessel's equation. This well-known second-order differential equation has two independent solutions. Numerous cylinder functions, as illustrated in App. 1, satisfy Bessel's equation. Energy considerations will dictate the choice of the functions selected as solutions of Eq. (5-9), that is,

1. The field must be finite in the core of the fiber. Specifically the cylinder function chosen in the core of the fiber must be finite at  $r = 0$ .
2. The field in the cladding of the fiber must have an exponentially decaying behavior at large distances from the center of the fiber.

### 5-3 THE FIELDS IN THE CORE AND CLADDING OF THE STEP-INDEX FIBER

To obtain the proper field configurations in the round optical fiber, one must select the appropriate cylinder function solutions of Bessel's equation—(5.9)—in the core, and the cladding that satisfy the physical requirements listed in Sec. 2.

Since the fields must be finite at the center of the fiber core, we will choose  $J_v(\kappa r)$  (see App. 1) as the form of the solution for  $r < a$ . Therefore, for  $r < a$

$$E_z = AJ_v(\kappa r)e^{iv\phi} \quad (5-10)$$

$$H_z = BJ_v(\kappa r)e^{iv\phi} \quad (5-11)$$

We require that the field in the cladding of the fiber decay in the  $r$  direction and be of the form  $e^{-\gamma r}$ .

If we define  $\kappa = j\gamma$  we can choose a modified Hankel function of the first kind as shown in App. 1, to describe the decaying behavior of the field in the cladding for large  $r$ .

That is, for  $r > a$

$$E_z = CH_v^{(1)}(j\gamma r)e^{iv\phi} \quad (5-12)$$

$$H_z = DH_v^{(1)}(j\gamma r)e^{iv\phi} \quad (5-13)$$

where  $A, B, C, D$  are unknown constants.

To obtain the transverse fields in the core and cladding of the guide, one must use Eqs. (3-23) to (3-26).

For example, to obtain  $E_r$ , one must differentiate the longitudinal fields with respect to  $r$  and  $\phi$ .

$$E_r = \frac{-j}{\kappa^2} \left( \beta \frac{\partial E_z}{\partial r} + \omega\mu \frac{1}{r} \frac{\partial H_z}{\partial \phi} \right) \quad (5-14)$$

In the core for  $r < a$

$$\frac{\partial E_z}{\partial r} = A\kappa J'_v(\kappa r)e^{iv\phi} \quad (5-15)$$

where

$$J'_v(\kappa r) = \frac{\partial J_v(\kappa r)}{\partial (\kappa r)} \quad (5-16)$$

$$\frac{\partial H_z}{\partial \phi} = B(j\gamma)J_v(\kappa r)e^{iv\phi} \quad (5-17)$$

Substituting Eqs. (5-15) and (5-17) into Eq. (5-14) results in

$$E_r = \frac{-j}{\kappa^2} \left[ A\beta\kappa J'_v(\kappa r)e^{iv\phi} + B(j\gamma)\omega\mu \frac{1}{r} J_v(\kappa r)e^{iv\phi} \right] \quad (5-18)$$

In a similar way using Eqs. (3-24) to (3-26) one can obtain

$$E_\phi = \frac{-j}{\kappa^2} \left[ j\beta \frac{v}{r} AJ_v(\kappa r) - \kappa\omega\mu BJ'_v(\kappa r) \right] e^{iv\phi} \quad (5-19)$$

$$H_r = \frac{-j}{\kappa^2} \left[ -j\omega\varepsilon_1 \frac{v}{r} AJ_v(\kappa r) + \kappa\beta BJ'_v(\kappa r) \right] e^{iv\phi} \quad (5-20)$$

and

$$H_\phi = \frac{-j}{\kappa^2} \left[ \kappa\omega\varepsilon_1 AJ'_v(\kappa r) + j\beta \frac{v}{r} BJ_v(\kappa r) \right] e^{iv\phi} \quad (5-21)$$

where

$$\kappa^2 = k_1^2 - \beta^2 \quad (5-22)$$

$$k_1^2 = \omega^2\mu_0\varepsilon_1 \quad (5-23)$$

The transverse fields in the cladding of the fiber can be obtained in the same fashion by differentiating Eqs. (5-12) and (5-13) with respect to  $r$  and  $\phi$  and substituting into Eqs. (3-23) to (3-26). If one goes through this exercise one obtains for  $r > a$

$$E_r = \frac{-1}{\gamma^2} \left[ \beta\gamma CH_v^{(1)\prime}(j\gamma r) + \omega\mu_0 \frac{v}{r} DH_v^{(1)}(j\gamma r) \right] e^{iv\phi} \quad (5-24)$$

$$E_\phi = \frac{-1}{\gamma^2} \left[ \beta \frac{v}{r} CH_v^{(1)}(j\gamma r) - \gamma\omega\mu_0 DH_v^{(1)}(j\gamma r) \right] e^{iv\phi} \quad (5-25)$$

$$H_r = \frac{-1}{\gamma^2} \left[ -\omega\varepsilon_2 \frac{v}{r} CH_v^{(1)\prime}(j\gamma r) + \gamma\beta DH_v^{(1)\prime}(j\gamma r) \right] e^{iv\phi} \quad (5-26)$$

$$H_\phi = \frac{-1}{\gamma^2} \left[ \gamma\omega\varepsilon_2 CH_v^{(1)}(j\gamma r) + \beta \frac{v}{r} DH_v^{(1)}(j\gamma r) \right] e^{iv\phi} \quad (5-27)$$

where

$$\frac{\partial H_v^{(1)\prime}(j\gamma r)}{\partial (j\gamma r)} = H_v^{(1)\prime}(j\gamma r) \quad (5-28)$$

and

$$\gamma^2 = \beta^2 - k_2^2 \quad (5-29)$$

$$k_2^2 = \omega^2 \mu_0 \varepsilon_2 \quad (5-30)$$

The total field configurations in the round optical fiber are described by Eqs. (5-18) to (5-21) and (5-24) to (5-27). The constants  $A$ ,  $B$ ,  $C$ ,  $D$ , and  $\beta$  will be determined by applying the boundary conditions for the two tangential components of the electric and magnetic fields at the core-cladding interface ( $r = a$ ).

#### 5-4 BOUNDARY CONDITIONS AND CHARACTERISTIC EQUATION FOR STEP-INDEX FIBER

The boundary conditions for the fields at the core-cladding interface ( $r = a$ ) can be written as

$$\left. \begin{aligned} Ez_1 &= Ez_2 \\ E\phi_1 &= E\phi_2 \\ Hz_1 &= Hz_2 \\ H\phi_1 &= H\phi_2 \end{aligned} \right\} r = a$$

where the subscripts 1 and 2 refer to the fields in the core and cladding respectively. Applying these conditions yields four simultaneous equations for the unknowns  $A$ ,  $B$ ,  $C$ , and  $D$ .

Using Eqs. (5-10) and (5-12) the boundary condition equation for  $E_z$  is,

$$J_v(\kappa a)A - H_v^{(1)}(j\gamma a)C = 0 \quad (5-31)$$

Substituting  $r = a$  into Eqs. (5-19) and (5-25) yields the equation for  $E_\phi$

$$\begin{aligned} \left( \frac{\beta}{\kappa^2 a} \right) J_v(\kappa a)A + j \frac{\omega \mu_0}{\kappa} J_v'(\kappa a)B \\ + \left( \frac{\beta}{\gamma^2 a} \right) H_v^{(1)}(j\gamma a)C - \frac{\omega \mu_0}{\gamma} H_v^{(1)}(j\gamma a)D = 0 \end{aligned} \quad (5-32)$$

From Eqs. (5-11) and (5-13) the boundary-condition equation for  $H_z$  is

$$J_v(\kappa a)B - H_v^{(1)}(j\gamma a)D = 0 \quad (5-33)$$

Finally using Eqs. (5-21) and (5-27) the resulting boundary condition equation for  $H_\phi$  is

$$\begin{aligned} \left( \frac{-j\omega \epsilon_1}{\kappa} \right) J_v'(\kappa a)A + \left( \frac{\beta}{\kappa^2 a} \right) J_v(\kappa a)B \\ + \left( \frac{\omega \epsilon_2}{\gamma} \right) H_v^{(1)}(j\gamma a)C + \left( \frac{\beta}{\gamma^2 a} \right) H_v^{(1)}(j\gamma a)D = 0 \end{aligned} \quad (5-34)$$

Equations (5-31) to (5-34) form a set of simultaneous equations that have a nontrivial solution provided that the system determinant for the four equations vanishes, that is,

$$\begin{vmatrix} J_v(\kappa a) & 0 & -H_v^{(1)}(j\gamma a) & 0 \\ \frac{\beta}{a \kappa^2} J_v(\kappa a) & \frac{j\omega \mu_0}{\kappa} J_v'(\kappa a) & \frac{\beta}{a \gamma^2} H_v^{(1)}(j\gamma a) & \frac{-\omega \mu_0}{\gamma} H_v^{(1)}(j\gamma a) \\ 0 & J_v(\kappa a) & 0 & -H_v^{(1)}(j\gamma a) \\ \frac{-j\omega \epsilon_1}{\kappa} J_v'(\kappa a) & \frac{\beta}{a \kappa^2} J_v(\kappa a) & \frac{\omega \epsilon_2}{\gamma} H_v^{(1)}(j\gamma a) & \frac{\beta}{a \gamma^2} H_v^{(1)}(j\gamma a) \end{vmatrix} = 0 \quad (5-35)$$

Expansion of this determinant results in what is known as the "eigenvalue" or characteristic equation of the waveguide. This equation defines the modes in the guide and yields the permissible values of  $\beta$ ,  $\kappa$ , and  $\gamma$  associated with each mode. In App. 2 the system determinant (5-35) is expanded and the resulting characteristic equation for the step-index fiber is

$$\begin{aligned} \left[ \frac{\epsilon_1}{\epsilon_2} \frac{\alpha y^2}{\kappa} J_v'(\kappa a) \right] \left[ \frac{\alpha y^2 J_v'(\kappa a)}{\kappa J_v(\kappa a)} + j\gamma a \frac{H_v^{(1)}(j\gamma a)}{H_v^{(1)}(j\gamma a)} \right] \\ = \left[ \sqrt{\left( \frac{\epsilon_1}{\epsilon_2} - 1 \right) \frac{\beta \kappa^2}{\kappa^2}} \right]^2 \end{aligned} \quad (5-36)$$

Although mathematically more complicated, Eq. (5-36) is conceptually similar to the characteristic equations derived in Chap. 4 for the dielectric slab waveguide. In the next section the characteristic equation (5-36) will be analyzed to determine the types of modes that exist in an optical fiber.

The coefficients in Eqs. (5-31) to (5-34) can be rewritten so that  $A$  is the only unknown coefficient. For example Eqs. (5-31) and (5-33) relate respectively  $A$  and  $C$  and  $B$  and  $D$  to each other.

$$C = \frac{J_v(\kappa a)}{H_v^{(1)}(j\gamma a)} A \quad (5-37)$$

$$D = \frac{J_v(\kappa a)}{H_v^{(1)}(j\gamma a)} B \quad (5-38)$$

The coefficients  $A$  and  $B$  are related to each other via Eqs. (5-32) or (5-34) using Eqs. (5-37), (5-38), and (5-34). Solving for  $B$  in terms of  $A$  yields<sup>1</sup>

$$B = \frac{j \arctan[\epsilon_1 \gamma J_v'(\kappa a) H_v^{(1)}(j\gamma a) + j \epsilon_2 \kappa J_v(\kappa a) H_v^{(1)}(j\gamma a)]}{\omega(\epsilon_1 - \epsilon_2) \mu_0 \beta J_v(\kappa a) H_v^{(1)}(j\gamma a)} A \quad (5-39)$$

If Eq. (5-32) were used instead of (5-34) the resulting relationship between  $B$  and  $A$  would be

$$B = j\gamma \frac{\omega(\epsilon_1 - \epsilon_2) \beta J_v(\kappa a) H_v^{(1)}(j\gamma a)}{\kappa \gamma a [j\gamma J_v'(\kappa a) H_v^{(1)}(j\gamma a) + j \kappa J_v(\kappa a) H_v^{(1)}(j\gamma a)]} A \quad (5-40)$$

Equations (5-39) and (5-40) will be used in Sec. 5-5 when we determine the types of modes that can propagate in a step-index fiber.

### 5-5 CHARACTERIZATION OF MODES IN A STEP-INDEX OPTICAL FIBER

In general the permissible field configurations or modes that exist in a step-index fiber have six field components. For the round fiber hybrid modes exist as well as the TE and TM modes that we observed in the dielectric slab waveguide. The hybrid modes will be denoted as HE and EH modes and have both longitudinal electric and magnetic field components present. In terms of a ray analogy for the step-index fiber, the hybrid modes correspond to propagating skew rays and the TE and TM modes to meridional rays. For the special case  $\nu = 0$ , only meridional rays propagate in the guide. For this case the right-hand side of the characteristic equation (5-36) is equal to zero and one obtains two characteristic equations that define the TE and TM modes. These equations are written below.

$$\begin{aligned} \left[ \frac{\alpha y^2}{\kappa} \frac{J'_0(\kappa a)}{J_0(\kappa a)} + j \gamma a \frac{H_0^{(1)}(j \gamma a)}{H_0^{(1)}(j \gamma a)} \right] &= 0 \\ \left[ \frac{\varepsilon_1 \alpha y^2}{\varepsilon_2} \frac{J'_0(\kappa a)}{J_0(\kappa a)} + \frac{j \gamma a H_0^{(1)}(j \gamma a)}{H_0^{(1)}(j \gamma a)} \right] &= 0 \end{aligned} \quad (5-41)$$

To understand that Eq. (5-41) is the defining equation for the TE modes and Eq. (5-42) the defining equation for the TM modes let us recall that for TE modes  $E_z = 0$  and for TM modes  $H_z = 0$ . Since

$$E_z = AJ_\nu(kr)e^{j\nu\phi} \quad (5-43)$$

and

$$H_z = BJ_\nu(kr)e^{j\nu\phi} \quad (5-44)$$

$E_z$  is equal to zero when  $A = 0$ , and  $H_z = 0$  when  $B = 0$ . Referring to Eq. (5-39) when  $\nu \rightarrow 0$ ,  $B \rightarrow \infty$  unless  $A = 0$ . Equation (5-41) is the characteristic equation for the guide when  $\nu \rightarrow 0$  and  $A = 0$ . That is, Eq. (5-41) is the defining equation for the TE modes. Using Eq. (5-40) when  $\nu = 0$ ,  $B = 0$ , Eq. (5-42) is the characteristic equation for the guide for the TM modes when  $\nu = 0$  and  $B = 0$ .

Equations (5-41) and (5-42) can be rewritten in a simpler way if we recall from Eq. (A1-19) that for any cylinder function

$$Z'_0 = -Z_1 \quad (5-45)$$

Then Eqs. (5-41) and (5-42) become,

$$\text{Defining equation for TE modes, } \frac{\gamma}{\kappa} \frac{J_1(\kappa a)}{J_0(\kappa a)} + j \frac{H_1^{(1)}(j \gamma a)}{H_0^{(1)}(j \gamma a)} = 0 \quad (5-46)$$

and,

$$\text{Defining equation for TM modes, } \frac{\varepsilon_1 \gamma}{\varepsilon_2 \kappa} \frac{J_1(\kappa a)}{J_0(\kappa a)} + j \frac{H_1^{(1)}(j \gamma a)}{H_0^{(1)}(j \gamma a)} = 0 \quad (5-47)$$

In summary the characteristic equation (5-36) defines the propagating modes in a step-index optical fiber. The solutions to this equation are, to say the least, extremely complicated and normally obtained numerically on a computer. The general solution for  $\nu \neq 0$  has six field components and defines the propagation conditions for the (HE, EH) hybrid modes. For the special case of  $\nu = 0$  we can derive two separate characteristic equations, (5-46) and (5-47), that describe the conditions for propagation of the TE and TM modes.

### 5-6 MODE CUTOFF CONDITIONS

An important parameter for each propagating mode is its cutoff frequency. As we have already discussed in Chap. 4, a mode is cut off when its field in the cladding ceases to be evanescent and is detached from the guide, that is, the field in the cladding does not decay. The rate of decay of the field in the cladding is determined by the value of the constant  $\gamma$ . In App. 1 we developed the expression for the asymptotic approximation of the modified Hankel function for large values of its argument<sup>5</sup>

$$H_\nu^{(1)}(j \gamma r) = \sqrt{\frac{2}{\pi j \gamma r}} (e^{-j(\pi \nu/2 + \pi/4)} e^{-\gamma r}) \quad (5-48)$$

For large values of  $\gamma$ , the field is tightly concentrated inside and close to the core. With decreasing values of  $\gamma$ , the field reaches farther out into the cladding. Finally, for  $\gamma = 0$ , the field detaches itself from the guide. The frequency at which this happens is called the cutoff frequency. At cutoff

$$\gamma = 0 = \sqrt{\beta_c^2 - k_{2c}^2} \quad (5-49)$$

or

$$\beta_c^2 = k_{2c}^2 \quad (5-50)$$

where

$$k_{2c}^2 = \omega_c^2 \mu_0 \varepsilon_2 \quad (5-51)$$

In the core of the guide at cutoff we have

$$\kappa_c^2 = k_{1c}^2 - \beta_c^2 \quad (5-52)$$

$$k_{1c}^2 = \omega_c^2 \mu_0 \varepsilon_1 \quad (5-53)$$

We can obtain an expression for the cutoff frequency of a mode by substituting Eq. (5-50) into (5-52)

$$\kappa_c^2 = k_{1c}^2 - k_{2c}^2 = \omega_c^2 \mu_0 (\varepsilon_1 - \varepsilon_2) \quad (5-54)$$

Solving for  $\omega_c$  from Eq. (5-54)

$$\omega_c = \frac{\kappa_c}{\sqrt{\mu_0(\epsilon_1 - \epsilon_2)}} \quad (5-55)$$

The cutoff frequency of a mode can be zero if  $\kappa_c = 0$ . One, and only one, mode can exist in an optical fiber with  $\omega_c = 0$ . This mode is the hybrid  $HE_{11}$  mode which exists for all frequencies. It is therefore possible to design and operate a single-mode optical fiber. The single-mode fiber has a very small core diameter and small refractive index difference between the core and cladding. These parameters must be chosen to ensure that all other guided modes are below their cutoff frequency. Before we can develop the design equation for a single-mode fiber, we must develop the equations for the cutoff conditions (and solve for the  $\kappa_c$ 's) for the different types of modes that can exist in a step-index optical fiber.

In App. 3 the characteristic equation (5-36) has been reworked for convenient solution at mode cutoff. By allowing  $\gamma$  to approach zero, and using an approximation for the modified Hankel function for small arguments, we obtain the following mode cutoff conditions.

#### TE and TM modes $v = 0$

The cutoff conditions for the  $TE_{0\mu}$  and  $TM_{0\mu}$  modes are obtained from the  $\mu$ th roots of Eq. (5-56) shown below

$$J_0(\kappa a) = 0 \quad (5-56)$$

That is, the value of  $\kappa_c a$  is obtained from the roots of Eq. (5-56), as shown in Fig. 5-2. The corresponding cutoff frequency for a mode is calculated using this value of  $\kappa_c$  in Eq. (5-55).

#### Hybrid Modes

##### $HE_{1\mu}$ modes

The cutoff condition of the  $HE_{1\mu}$  modes is described by Eq. (5-57)

$$\kappa_c a = x_{v\mu} \quad \text{for } v = 1, 2, 3, \dots \quad (5-57)$$

where the parameter  $x_{v\mu}$  is the  $\mu$ th root of the equation

$$J_v(x_{v\mu}) = 0 \quad (5-58)$$

As previously discussed the fundamental or  $HE_{11}$  mode exists for all frequencies. It will propagate when all other modes are cut off. The equation that describes its cutoff condition is:

##### $HE_{11}$ mode

$$\kappa_c a = 0 \quad (5-59)$$

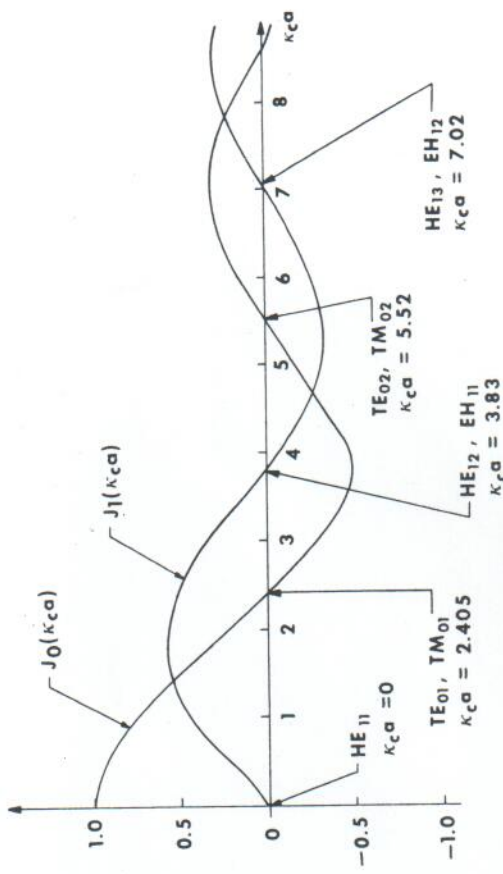


Figure 5-2 Plot of Bessel functions used for calculating cutoff conditions of modes.

**EH<sub>vμ</sub> modes** The cutoff condition equation for the  $EH_{v\mu}$  modes is also Eq. (5-58) but with the added constraint  $x_{v\mu} \neq 0$ .

Figure 5-2 shows a graphical example of how to calculate the cutoff condition for the  $HE_{1\mu}$  and  $EH_{1\mu}$  modes. Finally, the remaining  $HE_{v\mu}$  modes have the following cutoff condition equation that must be solved.

$$HE_{v\mu} \text{ modes} \quad \text{for } v = 2, 3, 4, \dots$$

$$\left( \frac{\epsilon_1}{\epsilon_2} + 1 \right) J_{v-1}(\kappa_c a) = \frac{a\kappa_c}{v-1} J_v(\kappa_c a) \quad (5-60)$$

For the hybrid modes there are two types of modes for each integral value of  $v > 1$ . The modes whose cutoff frequency is determined by Eq. (5-58) are designated  $EH_{v\mu}$  modes. Equation (5-60) determines the cutoff frequencies of the  $HE_{v\mu}$  modes. Both the  $EH_{1\mu}$  and  $HE_{1(v+1)\mu}$  modes have the same cutoff frequency. However, they are not degenerate modes since at frequencies other than cutoff, they have different propagation constants. For  $v = 0$  we have the nondegenerate TE and TM modes, whose identical cutoff condition is given by Eq. (5-56). One can calculate the cutoff parameter  $\kappa_c a$  for the different types of modes that exist in a step-index fiber from Eqs. (5-56) to (5-60). Table 5-2 lists the first few low-order modes and their respective cutoff parameter values. To calculate the cutoff parameter for the  $HE_{v\mu}$  modes (Eq. (5-60)) a knowledge of the ratio of the refractive indices of the core and cladding of the fiber is required. The cutoff parameters for all the other modes are obtained directly, for a given order  $v$  and

Table 5-2

Mode	Cutoff parameter, $\kappa_c a$	Mode	Cutoff parameter, $\kappa_c a$
$HE_{11}$	0.0	$EH_{31}$	6.38
$TE_{01}, TM_{01}$	2.405	$E_{51}$	6.41
$HE_{21}$	2.42	$HE_{13}, EH_{12}$	7.02
$HE_{12}, EH_{11}$	3.83	$HE_{32}$	7.02
$HE_{31}$	3.86	$EH_{41}$	7.59
$EH_{21}$	5.14	$HE_{61}$	7.61
$HE_{41}$	5.16	$EH_{22}$	8.42
$TE_{02}, TM_{02}$	5.52	$HE_{32}$	8.43
$HE_{22}$	5.53		

corresponding root  $\mu$ , from the Bessel functions. It is assumed in Table 5-2 that  $n_1/n_2 = 1.02$  ( $f_1/f_2 = 1.0404$ )

$$n_1/n_2 = 1.02, (\varepsilon_1/\varepsilon_2 = 1.0404.)$$

To appreciate the significance of the cutoff parameter  $\kappa_c a$  let us define it in terms of the physical parameters of the fiber. From Eq. (5-54)

$$K(\theta) = \sqrt{1 - \frac{\theta}{\theta_0}} \left( \sqrt{n^2 - n^2} \right)$$

noticing that

$$\omega_c \sqrt{\mu_0 \varepsilon_0} = \frac{2\pi}{l} \quad (5-62)$$

$$V \equiv \kappa_c a = \frac{2\pi a}{j_1} \sqrt{n_1^2 - n_2^2} \quad (5-63)$$

The cutoff parameter  $\kappa_c a$  is usually called the "V" number of the fiber. Notice that the V number for the fiber is analogous to the parameter  $R$  for the dielectric slab waveguide. The number of propagating modes in the step-index fiber is proportional to its V number. Table 5-3 illustrates how increasing  $a$ ,  $n_1$ ,  $n_2$ , or  $\lambda_0$  influences the number of propagating modes in the fiber.

Table 2

Increasing physical parameter	Number of propagating modes
Core radius $a$	Increases
Core refractive index, $n_1$	Increases
Cladding refractive index, $n_2$	Decreases
Source wavelength, $\lambda_0$	Decreases

**Example 5.1 Multimode step-index fiber** We wish to design a multimode step-index fiber with a V number,  $V = 100$  and a numerical aperture,  $NA = 0.30$ . This fiber will be used in a data link with a  $0.82 \mu\text{m}$  light-emitting diode (LED) source. We will determine the fiber parameters  $a$ ,  $n_1$ , and  $n_2$ , as follows.

$$V = \frac{2\pi a}{i} \sqrt{n_1^2 - n_2^2}$$

$$NA = \sqrt{n_1^2 - n_2^2}$$

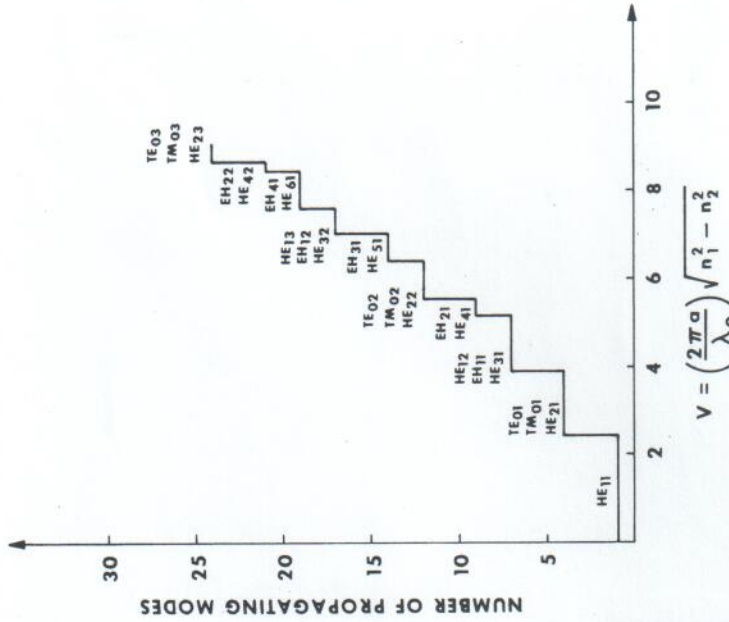


**Figure 5.3** Plot of number of propagating modes vs fiber V number.

Choose a fused silica core  $n_1 = 1.458$ .

$$n_2 = \sqrt{n_1^2 - NA^2} \\ = 1.427$$

$$a = \frac{\lambda_0 V}{2\pi(NA)} \\ = 43.5 \mu\text{m}$$

The fiber design is

$$a = 43.5 \mu\text{m}$$

$$n_1 = 1.458$$

$$n_2 = 1.427$$

To fully design the fiber we would also need to specify a value for the cladding radius  $b$  which would ensure that the evanescent fields in the cladding approach zero before the cladding-air interface. A typical cladding radius that satisfies this requirement is:

$$b = 62.5 \mu\text{m}$$

### 5-7 SINGLE-MODE OPTICAL FIBER

In this section we will develop an equation and use it to design a single-mode step-index fiber. Recall from Fig. 5-3 that the number of propagating modes in a step-index fiber is a function of its  $V$  number. For  $V < 2.405$  the only mode that propagates in a fiber is the fundamental  $HE_{11}$  mode. To develop the design equation for a single-mode fiber let us rewrite Eq. (5-63) in terms of  $\Delta$ , the fractional refractive index difference between the core and cladding

$$V = \frac{2\pi a}{\lambda_0} \sqrt{n_1^2 - n_2^2} = \frac{2\pi a}{\lambda_0} n_1 \sqrt{2\Delta - \Delta^2} \quad (5-64)$$

where

$$n_2 = n_1(1 - \Delta) \quad (5-65)$$

and

$$\Delta = \frac{n_1 - n_2}{n_1} \quad (5-66)$$

for small  $\Delta$ ,  $\Delta^2 \ll 2\Delta$  and Eq. (5-64) becomes

$$V \approx \frac{2\pi a}{\lambda_0} \sqrt{2} n_1 \sqrt{\Delta} = 8.886 \frac{an_1}{\lambda_0} \sqrt{\Delta} \quad (5-67)$$

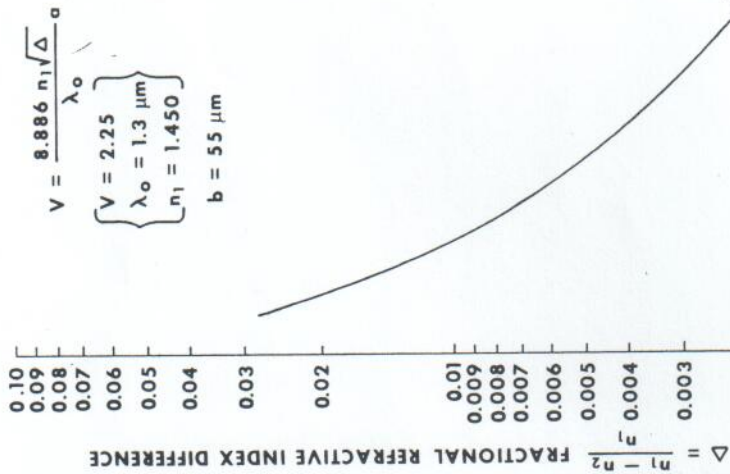


Figure 5-4 Design curve for single-mode fiber.

Using Eq. (5-67) we can design a single mode if  $V < 2.405$ . Let us assume the following values for our design:

$$V = 2.25 \\ \lambda_0 = 1.3 \mu\text{m} \\ n_1 = 1.450$$

Substituting these values into Eq. (5-67) we can obtain a design curve (Fig. 5-4) showing the relationship between  $\Delta$  and the core radius  $a$  for a

single-mode fiber. Referring to Fig. 5-4, we wish to choose the radius  $a$  large enough to make the splicing of single-mode fibers a viable task. We must also choose  $\Delta$  large enough to make the fiber manufacturable. We are free to choose a value for the cladding radius  $b$ . Our choice will be made to ensure that the power in the evanescent cladding field approaches zero at the outside diameter of the fiber. With these considerations in mind, the following parameters for a single-mode fiber were chosen:

$$a = 5 \mu\text{m}$$

$$b = 55 \mu\text{m}$$

$$\Delta = 0.002$$

$n_1 = 1.450$  (refractive index of high-silica glass at  $\lambda = 1.3 \mu\text{m}$ )

**Example 5-2 Cutoff wavelength of a single-mode guide** Let us determine the cutoff wavelength, for single-mode operation, of the guide designed in Sec. 5.7 ( $a = 5 \mu\text{m}$ ,  $n_1 = 1.450$ ,  $\Delta = 0.002$ ).

If the  $V$  number of the fiber is greater than 2.405, the fiber will support more than one mode. We will calculate the cutoff wavelength for single-mode operation as follows:

$$V = 2.405 = \frac{2\pi a}{\lambda_0} \sqrt{n_1^2 - n_2^2}$$

Solving for  $\lambda_0$

$$2.405 = \frac{2\pi(5 \mu\text{m})}{\lambda_0} \sqrt{(1.450)^2 - (1.447)^2}$$

$$\lambda_0 = 1.218 \mu\text{m}$$

If  $\lambda_0$  is less than  $1.218 \mu\text{m}$  the guide will support more than one mode.

width) in the time domain (see Chap. 8). Since most applications of fibers in communication systems use some form of digital envelope modulation of an optical signal, the fiber performance is usually characterized in the time domain in terms of the degradation of an optical pulse propagating through the fiber (impulse response). In this section we will follow this practice by describing the mechanisms that cause the degradation of the shape of an optical pulse (group delay distortion) as it propagates through a single-mode fiber. The two mechanisms that contribute to delay distortion are: (1) chromatic (material) dispersion and (2) waveguide dispersion. Chromatic dispersion is the dominant effect and is a result of the fact that the group delay of an optical wave propagating in a glass medium is wavelength-dependent. Let us now develop the expression for group delay due to chromatic dispersion in a single-mode optical fiber.

If you recall from Chap. 2, the group delay of a mode is given by

$$\tau_g = \frac{1}{v_g} = \frac{N_g}{c} \quad (5-68)$$

where  $N_g$  is the group index of the medium

$$N_g = n - \lambda_0 \frac{dn}{d\lambda_0} \quad (5-69)$$

Since the glass that is used in optical fibers is a dispersive medium, the refractive index of the core of a single-mode fiber is dependent upon the communication system source wavelength  $\lambda_0$ . Suppose that the system source has a relative spectral bandwidth  $\Delta\lambda/\lambda$

$$\text{Relative spectral bandwidth of source} \equiv \frac{\Delta\lambda}{\lambda_0} \quad (5-70)$$

where  $\Delta\lambda = \lambda_2 - \lambda_1$  is a spread of wavelengths about a center wavelength  $\lambda_0$ .

Now consider that energy is propagating in a range of wavelengths  $\Delta\lambda$  in a single-mode fiber. If the energy propagates a distance  $L$  in the fiber, the spread in the arrival times of energy propagating at the different wavelengths  $\lambda_1$  and  $\lambda_2$  is

$$\Delta\tau_c = \frac{L}{c} N_g(\lambda_1) - \frac{L}{c} N_g(\lambda_2) \\ = -\frac{L}{c} \frac{dN_g}{d\lambda} \Delta\lambda \quad (5-71)$$

Using Eq. (5-69)

$$\frac{dN_g}{d\lambda} = \frac{dn_1}{d\lambda} - \lambda \frac{d^2n_1}{d\lambda^2} - \frac{dn_1}{d\lambda} \\ = -\lambda \frac{d^2n_1}{d\lambda^2} \quad (5-72)$$

When a very high-capacity optical communication system is designed, such as a transatlantic undersea link, the transmission medium used must have a bandwidth in excess of 10 GHz-km. Single-mode fibers would be the transmission medium of choice for this type of application because their bandwidths are very large and limited only by intramodal delay distortion (chromatic and waveguide dispersion). Single-mode fibers with measured bandwidths of 30 GHz- $\sqrt{\text{km}}$  have been reported in the literature.<sup>6</sup>

An optical fiber can be described in terms of its baseband frequency characteristic (bandwidth) or equivalently in terms of its impulse response (rms pulse

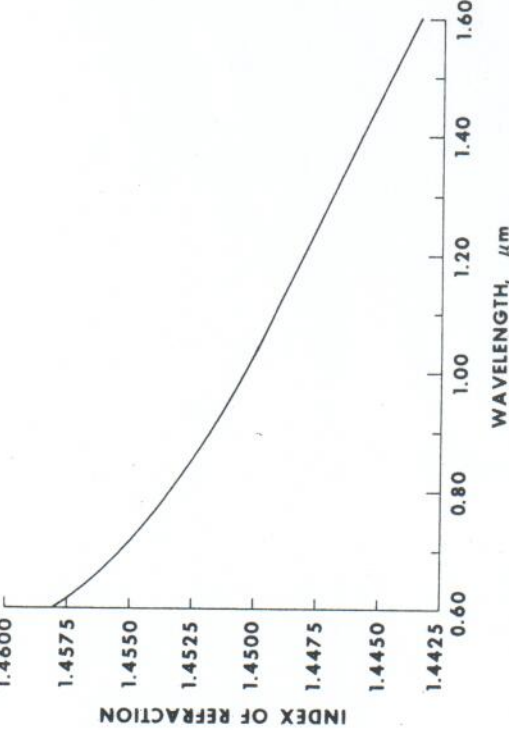


Figure 5-5 Refractive index of fused silica vs. wavelength.

and

$$\Delta\tau_e = \frac{L}{c} \lambda \frac{d^2 n_1}{d\lambda^2} \Delta\lambda \quad (5-73)$$

Writing Eq. (5-73) in terms of the relative bandwidth of the source

$$\Delta\tau_e = \frac{L}{c} \left( \frac{\Delta\lambda}{\lambda_0} \right) \lambda_0^2 \frac{d^2 n_1}{d\lambda^2} \quad (5-74)$$

Equation (5-74) can be used to approximate the chromatic dispersion component of delay distortion in a single-mode fiber. Figures 5-5 and 5-6 show respectively  $n_1$ <sup>7</sup> and  $\lambda^2(d^2 n_1/d\lambda^2)$  versus  $\lambda$  for fused silica.

To obtain an estimate of pulse broadening due to chromatic dispersion let us consider a GaAs laser operating at  $\lambda_0 = 0.82 \mu\text{m}$  with a linewidth  $\Delta\lambda = 1 \text{ nm}$ . The source relative bandwidth is  $\Delta\lambda/\lambda = 0.12$  percent.

Using Fig. 5-6 and Eq. (5-74) the pulse broadening due to chromatic dispersion for a kilometer of fiber would be approximately 100 ps. This effect can be substantially reduced if sources are operated at longer wavelengths. Referring to Fig. 5-6, in the region  $\lambda = 1.2 \mu\text{m}$  to  $1.4 \mu\text{m}$ ,

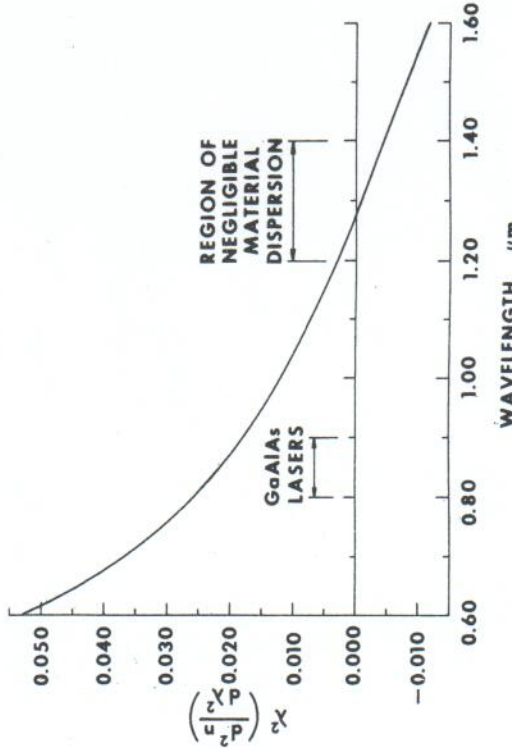
$$\lambda^2 \frac{d^2 n}{d\lambda^2} \approx 0 \quad (5-75)$$

This indicates that it is theoretically possible to find a source-wavelength region where pulse-spreading due to chromatic dispersion approaches zero. Experimental evidence<sup>8,9</sup> suggests that for germanium- or phosphorus-doped silica fibers the zero material dispersion region would occur at a longer wavelength than Fig. 5-6 suggests.

Let us now consider waveguide dispersion, the second mechanism that can cause some pulse broadening in a single-mode fiber. Waveguide dispersion is a result of the fact that the propagating characteristics of the mode are a function of the ratio between the core radius and the wavelength. An expression for waveguide dispersion has been developed in the literature.<sup>3,10</sup> It is presented here to give the reader an understanding of the size of the contributions to the total pulse-broadening due to this mechanism

$$\Delta\tau_w = \frac{L}{c} \left( \frac{\Delta\lambda}{\lambda} \right) (n_2 - n_1) D_w V \quad (5-76)$$

$D_w(V)$  is a dimensionless dispersion coefficient that is a function of the  $V$  number of the fiber. A plot of  $D_w(V)$  versus  $V$  is shown in Fig. 5-7. For the fiber parameters of the single-mode fiber designed in Sec. 5-7, and assuming a source linewidth  $\Delta\lambda = 1 \text{ nm}$ , the pulse-broadening due to waveguide dispersion is approximately two picoseconds for a kilometer of fiber, a very small part of the total pulse-broadening due to intramodal delay distortion in an optical fiber.

Figure 5-6  $\lambda^2(d^2 n/d\lambda^2)$  vs. wavelength showing zero material dispersion region.

the simplified characteristic equation by setting  $n_1 = n_2$  ( $\epsilon_1 = \epsilon_2$ ). Equation (5-77) becomes

$$(J^- - H^-)(J^+ - H^+) = 0 \quad (5-78)$$

Using Eqs. (A3-2) to (A3-5) we immediately obtain the two characteristic equations

$$\frac{J_{v-1}(ka)}{\kappa a J_v(ka)} = \frac{H_{v-1}^{(1)}(j\gamma a)}{j\gamma a H_v^{(1)}(j\gamma a)} \quad \text{for HE modes} \quad (5-79)$$

$$\frac{J_{v+1}(ka)}{\kappa a J_v(ka)} = \frac{H_{v+1}^{(1)}(j\gamma a)}{j\gamma a H_v^{(1)}(j\gamma a)} \quad \text{for EH modes} \quad (5-80)$$

The approximate characteristic equations (5-79) and (5-80) are much more convenient for obtaining solutions for the propagation constants than the exact characteristic equation (5-36). Marcuse<sup>1</sup> has shown that approximate expressions for the fields far from cutoff can be written in cartesian coordinates. The interested reader should refer to Marcuse's excellent book for the details of the derivation of these approximate fields. A further simplification of the approximate fields can be made if we realize that the HE modes of order  $v = v' + 1$  are almost degenerate with the EH modes of order  $v = v' - 1$ . Linear superposition of an HE and a EH mode results in a linearly polarized (LP) mode<sup>1,11,13</sup> that has only four field components. These new modes are much simpler in structure than the original HE and EH modes that have six field components. It is important to keep in mind that LP modes are not exact modes of the step-index fiber. Since the parent HE and EH modes have slightly different propagation constants as a function of  $z$  (degeneracy between the modes is not exact), the superposition of these modes changes with  $z$ . Therefore LP modes are not true modes but are useful and allow us to visualize the field structures of a step-index fiber in a simpler way.

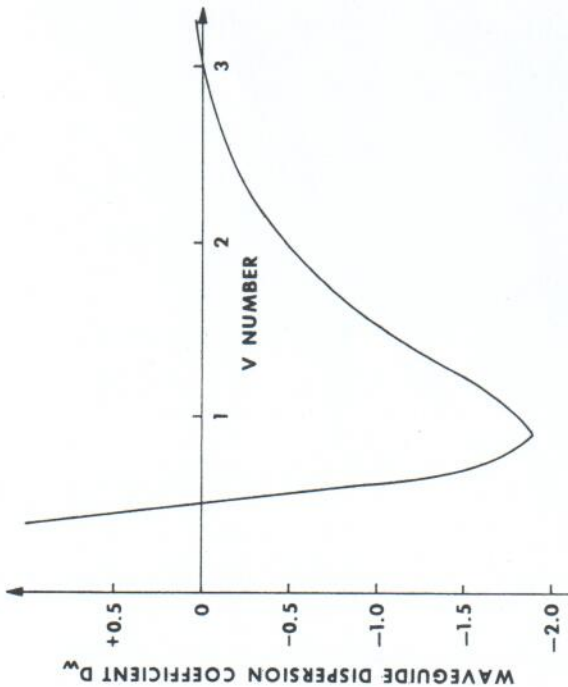


Figure 5-7 Plot of waveguide dispersion coefficient,  $D_w$  vs. V number.

### 5.9 WEAKLY GUIDING FIBERS; SIMPLIFIED CHARACTERISTIC EQUATION

In Secs. 5-4 and 5-5 we obtained a rigorous solution for the fields in a step-index fiber. Unfortunately the characteristic equation and the description of the six component hybrid fields obtained from this analysis was mathematically very complicated. To proceed farther with our analysis of a fiber with many modes would be an extremely difficult task unless some simplifying assumptions can be made. The simplification in the descriptions of the modes in a fiber is made possible by realizing that most fibers used for practical telecommunication applications have core materials whose refractive index is only slightly higher than that of the surrounding cladding, that is, we will assume that  $\Delta \ll 1$  and typically  $\Delta$  is less than 0.05. By making this assumption, considerable analytical simplifications result. In this section we will make use of the assumption  $\Delta \ll 1$  to derive the simplified characteristic equation for a weakly guiding fiber.

Starting with the exact characteristic equation (A3-8) for the step-index fiber

$$\left( \frac{\epsilon_1}{\epsilon_2} J^- - H^- \right) (J^+ - H^+) + \left( \frac{\epsilon_1}{\epsilon_2} J^+ - H^+ \right) (J^- - H^-) = 0 \quad (5-77)$$

where  $J^+$ ,  $J^-$ ,  $H^+$ , and  $H^-$  are defined by Eqs. (A3-2) to (A3-5). We can obtain

We begin our analysis of the LP modes by drawing an analogy with the slab waveguide studied in Chap. 4. If you recall, we reduced the slab waveguide to a two-dimensional problem with the symmetry restriction  $\partial/\partial y = 0$ . This resulted in a separation of the solution into TE modes ( $E_y$ ,  $H_x$ , and  $H_z$  field components) and TM modes ( $E_x$ ,  $E_z$ , and  $H_y$  field components). By analogy the three-dimensional fiber solution can be simplified by assuming  $\Delta \ll 1$ . The waves in the structure propagate at small angles to the axis and we can construct modes whose transverse fields are essentially polarized in one direction ( $E_y$ ,  $H_x$ ,  $E_z$ , and  $H_z$  field components or the orthogonal polarization where the field components are  $E_x$ ,  $H_y$ ,  $E_z$ , and  $H_z$ ).

Let us postulate transverse field components in a weakly guiding fiber as follows: in the core  $r < a$

$$E_y = \frac{\eta_0}{n_1} H_x = \frac{AJ_l(kr)}{J_l(U)} \cos l\phi \quad (5-81)$$

and in the cladding  $r > a$

$$E_y = \frac{\eta_0}{n_2} H_x = \frac{AH_l^{(1)}(jyr)}{H_l^{(1)}(jW)} \cos l\phi \quad (5-82)$$

where  $l = 0, 1, 2, 3, \dots$

$A$  is the electric field strength at the core-cladding interface  
 $\eta_0 = \sqrt{\mu_0/\epsilon_0}$  is the characteristic impedance of free space, and

$$U = ka \quad (5-83)$$

$$W = ya \quad (5-84)$$

$$V^2 = U^2 + W^2 \quad (5-85)$$

The longitudinal components  $E_z$  and  $H_z$  can be obtained from  $H_x$  and  $E_y$  using Eqs. (3-6c) and (3-7c). Rewriting these equations in terms of  $\eta_0$  we obtain

$$E_z = \frac{j\eta_0}{k_0 n_1^2} \frac{\partial H_x}{\partial y} \quad \text{in core of fiber} \quad (5-86)$$

$$E_z = \frac{j\eta_0}{k_0 n_2^2} \frac{\partial H_x}{\partial y} \quad \text{in cladding of fiber} \quad (5-87)$$

and

$$H_z = \frac{j}{k_0 \eta_0} \left( \frac{\partial E_y}{\partial x} \right) \quad \text{in the core and cladding of the fiber} \quad (5-88)$$

For the interested reader expressions for  $E_z$ ,  $H_z$ ,  $E_\phi$  and  $H_\phi$  are obtained in App. 4. In addition the characteristic equation for the LP modes is derived by assuming  $n_1 = n_2$  and matching the tangential components of the fields at the core-cladding interface. The resultant characteristic equation is

$$U \left[ \frac{J_{l-1}(U)}{J_l(U)} \right] = jW \left[ \frac{H_{l-1}^{(1)}(W)}{H_l^{(1)}(jW)} \right] \quad (5-89)$$

This characteristic equation is much simpler than the exact characteristic equation (5-36) developed in Sec. 5-4. It has been shown<sup>11</sup> to be accurate to within one and ten percent for  $\Delta \leq 0.1$  and  $\Delta \leq 0.25$  respectively.

The approximate characteristic equations (5-79) and (5-80) can be shown to be equal to (5-89). To do this for example for the HE modes, we invert (5-79) and let  $v = v' + 1$ . After using the recursion relation (A1-20) and simplifying, Eq. (5-89) is obtained. For the EH modes we follow the same procedure but let  $v = v' - 1$ .

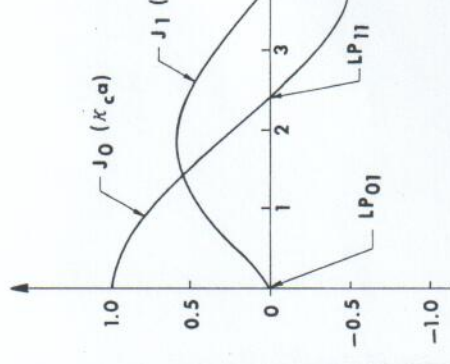


Figure 5-8 Plot of Bessel functions used for calculating cutoff conditions of  $LP_{0m}$  and  $LP_{1m}$  modes.

To obtain the cutoff condition for the LP modes, we require  $\gamma = 0$ . For the cutoff condition  $W = \gamma a = 0$  and the characteristic equation (5-89) becomes

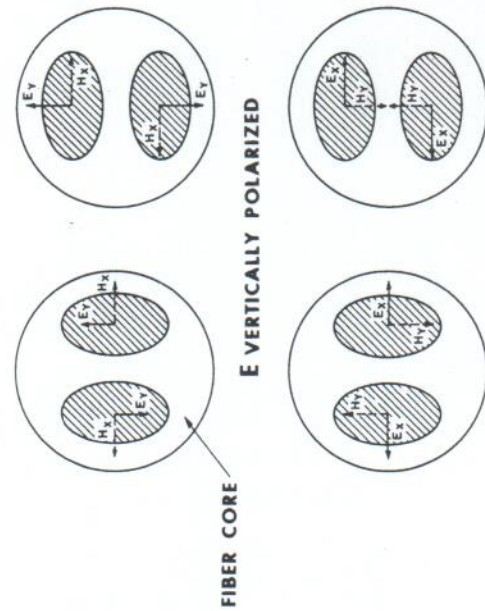
$$J_{l-1}(k_c a) = 0 \quad (5-90)$$

The lowest-order mode, characterized by  $l = 0$ , has a cutoff equation given by

$$J_1(k_c a) = -J_{-1}(k_c a) = 0 \quad (5-91)$$

This mode is labeled the  $LP_{01}$  mode having a field pattern described by  $l = 0$  and a cutoff characteristic of the first zero of the Bessel function. Referring to Fig. 5-8 the first zero occurs at  $k_c a = 0$ , that is the lowest-order mode cuts off only when  $a = 0$ . The  $LP_{01}$  mode corresponds to the fundamental  $HE_{11}$  mode obtained from the exact analysis of the fiber. The next mode of the  $l = 0$  type cuts off when  $J_1(k_c a)$  next equals zero, that is when  $k_c a = 3.83$ . This mode is called the  $LP_{02}$  mode. Similarly the modes characterized by  $l = 1$  have cutoffs when  $J_0(k_c a) = 0$ . Thus the  $LP_{11}$  mode cuts off when  $k_c a = 2.405$ . The notation for labelling the LP modes obviously is no longer the same as used for the exact solution since the integer  $l$  now refers to a superposition of exact modes with labels  $v + 1$  and  $v - 1$ . A comparison of the simplified-mode solutions with the exact modes shows that the  $LP_{lm}$  modes are actually a superposition of  $HE_{v+1,\mu}$  and  $EH_{v-1,\mu}$  modes.<sup>11,13</sup>

One of the attractive features of the LP mode theory is the ease with which we can visualize a mode. A complete set of modes exist in which only one electric and one magnetic field component are significant. The  $E$  vector can be chosen to lie along an arbitrary radius with the  $H$  vector along a perpendicular radius. Having made this choice there will always be a second independent polarization with the  $E$  and  $H$  vectors orthogonal to the first pair. Since each of

Figure 5-9 Four possible field distributions of  $LP_{11}$  mode.

the two possible polarization directions can be coupled with either a  $\cos l\phi$  or a  $\sin l\phi$  azimuthal dependence, four discrete mode patterns can be obtained from a single  $LP_{lm}$  label. Figure 5-9 illustrates four possible field distributions for the  $LP_{11}$  mode. We have previously noted that the  $LP_{lm}$  mode is formed from a linear combination of the  $HE_{v+1,\mu}$  mode and the  $EH_{v-1,\mu}$  mode, each of which has the possibility of a  $\cos l\phi$  or  $\sin l\phi$  dependence. Thus the new labeling system substitutes four LP mode patterns for four discrete HE and EH mode patterns, and each system forms a complete set.

and the characteristic equation becomes

$$U \frac{J_{l-1}(U)}{J_l(U)} = -W \quad (5-93)$$

The limiting value  $U = U_\infty$ , which is reached when  $W \rightarrow \infty$ , is given as the root of the equation

$$J_l(U_\infty) = 0 \quad (5-94)$$

For very large values of  $V$  we obtain an approximate value for the total number of modes by estimating the number of roots of the equation

$$J_l(U_m) = 0 \quad (5-95)$$

where

$$U_m \leq V$$

For large values of  $m$  an approximate formula for the roots of Eq. (5-95) is:<sup>14</sup>

$$U_m = (l + 2m - \frac{1}{2}) \frac{\pi}{2} \quad (5-96)$$

or approximately

$$U_m = (l + 2m) \frac{\pi}{2} \quad (5-97)$$

Referring to the mode-space diagram, Fig. 5-10, each point with integer coordinate values  $l$  and  $m$  represents one solution of Eq. (5-95) and is associated with one mode of a given polarization and  $\phi$  dependence. Each point can be thought of as representing a square of unit area in the mode-space diagram ( $l-m$  plane). The area in this space thus represents the number of modes. For constant values of  $U_m$ , the integer values of  $l$  and  $m$  satisfy Eq. (5-97) and lie along lines parallel to the dashed line shown in Fig. 5-11. Since the largest value of  $U_m$  is  $V$  the boundary for the modes in the mode-space diagram can be obtained by

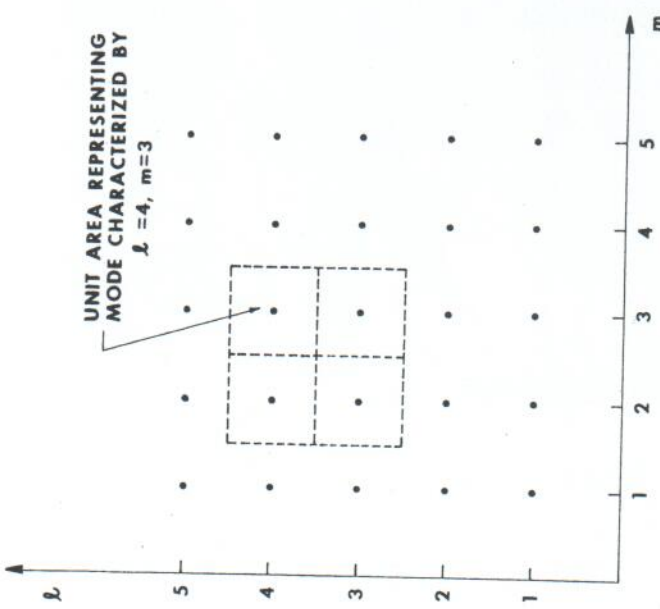
$$V = (l + 2m) \frac{\pi}{2} \quad (5-98)$$

## 5-11 TOTAL NUMBER OF MODES; PRINCIPAL MODE NUMBERS

It is often useful to be able to quickly estimate the total number of modes in a step-index fiber with a large  $V$  number. To develop this estimate we will approximate the characteristic equation (5-89) for tightly bound LP modes far from cutoff. Far from cutoff,  $W = \gamma a$  becomes large, and the asymptotic approximation for the modified Hankel functions (Eq. (5-48)) for large values of their arguments can be used in the characteristic equation (5-89), that is, for large  $\gamma$

$$\frac{H_{l-1}^{(1)}(jW)}{H_l^{(1)}(jW)} = \frac{\sqrt{2/j\pi W} e^{-j(l(l-1)(\pi/2) + \pi/4)}}{\sqrt{2/j\pi W} e^{-j(l(l(\pi/2) + \pi/4))}} e^{-W} = j \quad (5-92)$$

$$N = \frac{4V^2}{\pi^2} \quad (5-99)$$

Figure 5-10 Mode-space diagram, each point represents a mode in the  $l, m$  plane.

Equation (5-97) suggests that it is possible to associate a single-mode number, called the principal mode number, with all the modes characterized by the integer

$$M = l + 2m \quad (5-100)$$

The group of modes characterized by Eq. (5-100) form a degenerative mode group with the characteristic

$$\beta_M = \beta_{lm} \quad (5-101)$$

and have common cutoff values in the region of

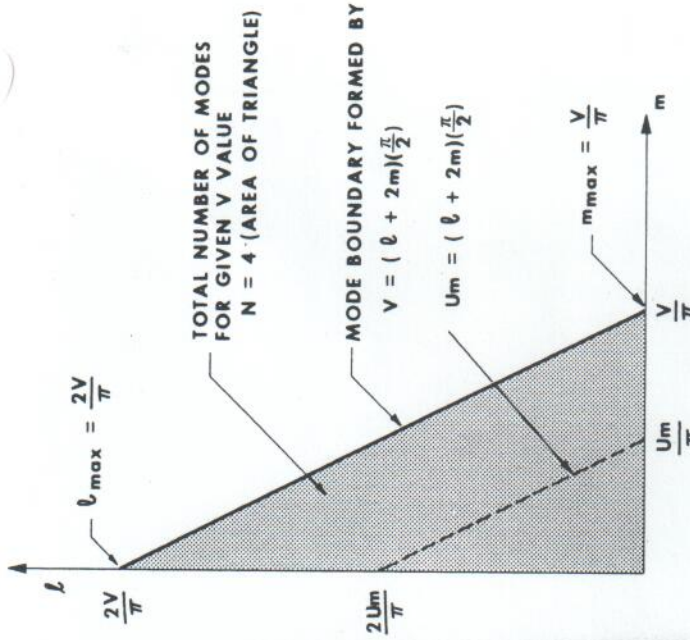
$$U = \frac{M\pi}{2} \quad (5-102)$$

We can write an expression for the total number of modes in terms of the maximum principal mode number  $M_{max}$ .

$$M_{max} = l_{max} + 2m_{max}$$

$$M_{max} = \frac{2V}{\pi} + \frac{2V}{\pi} = \frac{4V}{\pi} \quad (5-103)$$

$$k^2 = n_1^2 k_0^2 = \kappa^2 + \beta^2 \quad (5-107)$$

Figure 5-11 Mode-space diagram showing maximum boundary formed by  $V = (l + 2m)\pi/2$ .

Substituting Eq. (5-103) into (5-99) yields

$$N = \frac{M_{max}^2}{4} \quad (5-104)$$

In addition to being a convenient notational tool, the principal mode number  $M$ , can be related directly to the far-field angle of the radiation leaving a step-index fiber. The components of the propagation vector  $\vec{k}$  which defines the propagation direction of a mode (i.e., its representative plane wave) can be written in terms of  $M$  as follows:

$$\kappa = \frac{U}{a} = \frac{M\pi}{2a} \quad (5-105)$$

$$\beta = \sqrt{k^2 - \kappa^2} = \sqrt{k^2 - \frac{M^2\pi^2}{4a^2}} \quad (5-106)$$

where

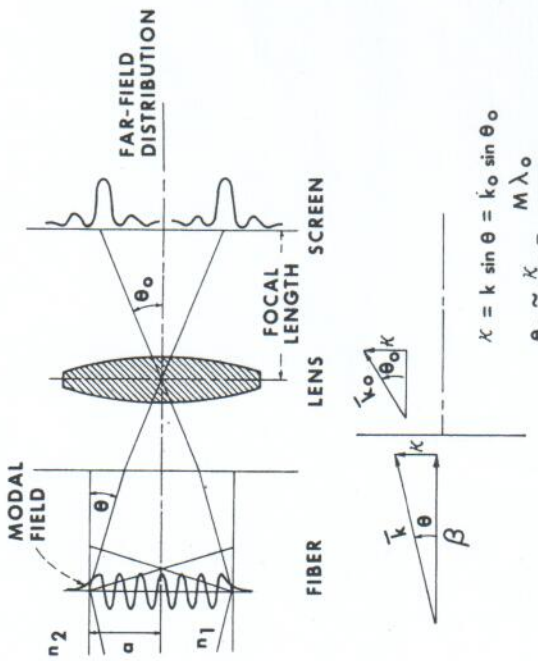
Figure 5-12 Relationship of far-field angle  $\theta_0$  and principal mode number,  $M$ .

Figure 5-12 illustrates that the transverse component of the propagation vector  $\kappa$  is conserved (by Snell's law) when the wave enters free space at the end of the waveguide, that is,

$$\kappa = k \sin \theta_1 = k_0 \sin \theta_0 \quad (5-108)$$

For weakly guiding fibers where the waves in the structure propagate at small angles to the axis,  $\sin \theta \approx \theta$ . Therefore in the far field (or the focal plane of the lens shown in Fig. 5-12) the wave will radiate into a cone of semiangle

$$\theta_0 = \frac{\kappa}{k_0} = \frac{(M\pi/2a)}{(2\pi/\lambda_0)} = \frac{M\lambda_0}{4a} \quad (5-109)$$

In the far field the angular concentration of the two far-field spots is about the directions  $+\theta_0$  and  $-\theta_0$ . The propagation directions of neighboring mode groups (for example mode groups  $M$  and  $M - 1$ ) differ by

$$\Delta\theta_0 = \frac{\lambda_0}{4a} \quad (5-110)$$

The mode groups thus form a partly overlapping sequence of spots in the far field, ordered according to principal mode number. Consequently the far-field distribution represents a direct image of the modal power distribution in a step-index fiber.<sup>15</sup>

## 5-12 POWER DISTRIBUTION IN A STEP-INDEX FIBER

In this section we will derive the distribution of the power that is carried by the guided modes in the core and in the cladding of a step-index fiber. By integrating the Poynting vector the amount of power contained in the core of the fiber is given by

$$P_{\text{core}} = \frac{1}{2} \int_0^{2\pi} \int_0^a r(E_x H_y^* - E_y H_x^*) dr d\phi \quad (5-111)$$

and the power in the cladding is given by

$$P_{\text{clad}} = \frac{1}{2} \int_0^{2\pi} \int_a^\infty r(E_x H_y^* - E_y H_x^*) dr d\phi \quad (5-112)$$

Using Eq. (5-81) to obtain  $E_y$  and  $H_x$  in the core and substituting into Eq. (5-111) yields

$$P_{\text{core}} = \frac{1}{2} \frac{A^2 n_1}{\eta_0 [J(\kappa r)]^2} \int_0^{2\pi} \int_0^a \cos^2[\phi J(\kappa r)]^2 dr d\phi \quad (5-113)$$

Integrating with respect to  $\phi$

$$P_{\text{core}} = \frac{\pi A^2 n_1}{2\eta_0 [J(\kappa r)]^2} \int_0^a [J(\kappa r)]^2 dr \quad (5-114)$$

and integrating with respect to  $r$

$$P_{\text{core}} = \frac{\pi n_1 A^2 a^2}{4\eta_0 [J(\kappa r)]^2} \{[J(\kappa r)]^2 - J_{l-1}(U)J_{l+1}(U)\} \quad (5-115)$$

To obtain the power in the cladding, Eq. (5-82) is substituted into Eq. (5-112). Upon integration with respect to  $r$  and  $\phi$ ,  $P_{\text{clad}}$  becomes

$$P_{\text{clad}} = \frac{\pi n_2 A^2}{4\eta_0 [H_l^1(jW)H_{l-1}^1(jW)]^2} \{H_{l+1}^1(jW)H_{l-1}^1(jW) - [H_l^1(jW)]^2\} \quad (5-116)$$

To simplify our notation, let

$$\alpha = \frac{[H_l^1(jW)]^2}{H_{l+1}^1(jW)H_{l-1}^1(jW)} \quad (5-117)$$

$$B = \frac{\pi n_2 A^2}{4\eta_0} \quad (5-118)$$

then

$$P_{\text{clad}} = B \left( \frac{1}{\alpha} - 1 \right) \quad (5-119)$$

Using the characteristic equations (A4-24) and (A4-25) we can rewrite  $P_{\text{core}}$  as

$$P_{\text{core}} = B \left[ 1 + \left( \frac{W}{U} \right)^2 \frac{1}{\alpha} \right] \quad (5-120)$$

The total power in the fiber is

$$P_{\text{tot}} = P_{\text{core}} + P_{\text{clad}} = \frac{B}{\alpha} \left[ 1 + \left( \frac{W}{U} \right)^2 \right] \quad (5-121)$$

and since  $V^2 = U^2 + W^2$

$$P_{\text{tot}} = \frac{B}{\alpha} \left( \frac{V^2}{U^2} \right) \quad (5-122)$$

To determine the fraction of the power in the core and cladding the following ratios are of interest

$$\frac{P_{\text{core}}}{P_{\text{tot}}} = \frac{B[1 + (W/U)^2] / \alpha}{B/\alpha[1 + (W/U)^2]} \quad (5-123)$$

Using  $W^2 = V^2 - U^2$  and simplifying yields

$$\frac{P_{\text{core}}}{P_{\text{tot}}} = 1 - \frac{U^2}{V^2} (1 - \alpha) \quad (5-124)$$

and

$$\frac{P_{\text{clad}}}{P_{\text{tot}}} = \frac{U^2}{V^2} (1 - \alpha) \quad (5-125)$$

An approximate expression for  $\alpha$  can be written as<sup>12</sup>

$$\alpha \approx 1 - (W^2 + l^2 + 1)^{-1/2} \quad (5-126)$$

For a mode close to cutoff,  $W \ll 1$  and  $U \approx V$

$$\begin{aligned} \alpha &\approx 1 - \frac{1}{\sqrt{l^2 + 1}} \\ \frac{P_{\text{core}}}{P_{\text{tot}}} &\approx 1 - \frac{1}{\sqrt{l^2 + 1}} \end{aligned} \quad (5-127) \quad (5-128)$$

and

$$\frac{P_{\text{clad}}}{P_{\text{tot}}} \approx \frac{1}{\sqrt{l^2 + 1}} \quad (5-129)$$

We see that for  $l = 0$  (a meridional mode) the mode's power moves into the cladding at cutoff. For highly skew modes ( $l \gg 0$ ), the power remains primarily concentrated in the core, even at cutoff. Figure 5-13 shows the ratio  $P_{\text{clad}}/P_{\text{tot}}$  for several modes as a function of the fiber V number.<sup>12</sup>

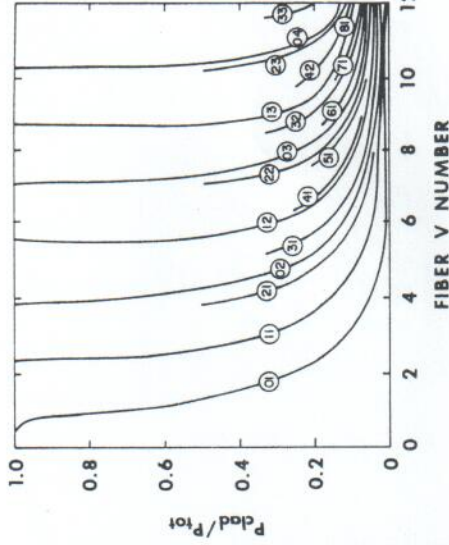


Figure 5-13 Plot of the ratio  $P_{\text{clad}}/P_{\text{tot}}$  vs. fiber V number.

### 5-13 DELAY DISTORTION IN A STEP-INDEX MULTIMODE FIBER

Pulse delay distortion in step-index multimode fibers is caused predominantly by the different group delays of the modes (modal delay distortion). This is the mechanism that limits the bandwidth of a step-index fiber and in turn the types of applications it can be used for in a communication system. We will now develop an expression for group delay  $\tau_g$  in a step-index fiber. Group delay determines the transit time of a pulse travelling through the fiber of length  $L$ . Using Eq. (4-109)

$$\tau_g = L \frac{d\beta}{d\omega} = \frac{L}{c} \frac{d\beta}{dk_0} = \frac{L}{c} \left( \frac{V}{k_0} \right) \frac{d\beta}{dV} \quad (5-130)$$

The equivalent forms of Eq. (5-130) are obtained from a knowledge of

$$k_0 = \frac{\omega}{c} \quad (5-131)$$

$$\frac{d\beta}{d\omega} = \frac{d\beta}{dk_0} \frac{dk_0}{d\omega} \quad (5-132)$$

$$\frac{dk_0}{d\omega} = \frac{1}{c} \quad (5-133)$$

$$V^2 = (n_1^2 - n_2^2)\alpha^2 k_0^2 \quad (5-134)$$

$$\frac{d\beta}{dk_0} = \frac{d\beta}{dV} \frac{dV}{dk_0} \quad (5-135)$$

and

$$\frac{dV}{dk_0} = \frac{V}{k_0} \quad (5-136)$$

We must now obtain an expression for  $\beta$  to substitute into the defining equation (5-130) for group delay. To be able to write  $\beta$  in a simple form let us define a normalized propagation constant  $b$  such that

$$b = \frac{W^2}{V^2} = \frac{(qa)^2}{V^2} \quad (5-137)$$

or

$$\gamma = \frac{V\sqrt{b}}{a} \quad (5-138)$$

for weakly guiding fibers  $\Delta = (n_1 - n_2)/n_2 \ll 1$ , Eq. (5-134) can be written as

$$V = \sqrt{2} n_2 k_0 a \sqrt{\Delta} \quad (5-139)$$

and

$$\gamma = n_2 k_0 \sqrt{2b\Delta} \quad (5-140)$$

We can now write  $\beta$  in a simplified form

$$\beta^2 = n_2^2 k_0^2 + \gamma^2 = n_2^2 k_0^2 (1 + 2\Delta b) \quad (5-141)$$

and

$$\beta \approx n_2 k_0 \sqrt{1 + 2\Delta b} \quad (5-142)$$

Using the expansion:

$$\sqrt{1+x} \approx 1 + \frac{x}{2} \quad \text{for } x \ll 1 \quad (5-143)$$

we obtain

$$\beta \approx n_2 k_0 (1 + \Delta b) \quad (5-144)$$

Substituting (5-144) into (5-130), the group delay becomes

$$\tau_g = \frac{L}{c} \frac{d(n_2 k_0)}{dk_0} + \frac{L}{c} \frac{V}{k_0} \frac{d}{dV} (n_2 k_0 \Delta b) \quad (5-145)$$

We can separate the group delay given by Eq. (5-145) as follows:

$$\tau_g = \tau_c + \tau_m \quad (5-146)$$

where

$$\tau_c = \frac{L}{c} \frac{d(n_2 k_0)}{dk_0} \equiv \text{modal delay characteristic of material (chromatic dispersion)} \quad (5-147)$$

$$\tau_m = \frac{L}{c} \frac{V}{k_0} \frac{d}{dV} (n_2 k_0 \Delta b) \equiv \text{modal waveguide delay} \quad (5-148)$$

$\tau_c$  is the group delay which is characteristic of the material of the fiber and is independent of a particular mode. Chromatic (material) dispersion is the mechanism that limits the bandwidth of single-mode fibers and is discussed in Sec. 5-8.

$\tau_m$ , the modal waveguide delay, is different for every mode. Consider a light pulse injected into and shared by many guided modes in the fiber. The light pulse will be split up into many pulses arriving at the end of the fiber at different times due to differences in the delays of the modes (modal delay distortion). We have encountered this phenomena before for the slab waveguide (Sec. 4-9). In order to obtain  $\tau_m$  we must use the characteristic equation (5-89), and can ultimately obtain the derivative with respect to  $V$  required in Eq. (5-148). For the interested reader, this procedure is followed in App. 5, and the arrival time difference between the mode with the largest waveguide group delay and the least delay is calculated. The resulting expression from App. 5 is

$$\Delta\tau_m = \frac{L}{c} n_1 - n_2 \left( 1 - \frac{\pi}{V} \right) \quad (5-149)$$

The difference  $\Delta\tau_m$  in the arrival times of the leading and trailing edge of the resultant output pulse of the fiber is given by Eq. (5-149). For a typical step-index fiber with the following parameters

$$a = 25 \mu\text{m}$$

$$\Delta = 0.01$$

$$L = 1 \text{ km}$$

$$\lambda_0 = 0.85 \mu\text{m}$$

$$V \approx 38$$

the modal pulse delay distortion  $\Delta\tau_m \approx 45 \text{ ns}$ .

Pulse distortion in step-index multimode fibers is caused predominantly by different group delays of the modes. Modal delay distortion is the primary mechanism that limits the use of step-index fibers to relatively low-bandwidth systems (less than 100 MHz-km). The contribution to the total delay distortion due to chromatic dispersion ( $\Delta\tau_c$ ) is much less than that due to modal delay distortion ( $\Delta\tau_m$ ). If the system source were a GaAs light-emitting diode with a relative bandwidth of four percent the delay distortion due to chromatic dispersion would be less than 5 ns.

**Example 5-3 Modal waveguide delay** Let us calculate the modal waveguide delay for 1 km of the multimode step-index fiber in Example 5-1.

$$\begin{aligned}\Delta\tau_m &= \frac{L}{c} (n_1 - n_2) \left(1 - \frac{\pi}{V}\right) \\ &= \frac{1 \text{ km}}{3 \times 10^8 \text{ m/s}} (1.458 - 1.427) \left(1 - \frac{\pi}{100}\right) \\ &= 100 \text{ ns}\end{aligned}$$

## REFERENCES

1. D. Marcuse: *Light Transmission Optics*, Van Nostrand Reinhold Co., New York, 1972.
2. J. E. Midwinter: *Optical Fibers for Transmission*, John Wiley and Sons, New York, 1979.
3. S. E. Miller and A. G. Chynoweth: *Optical Fiber Telecommunications*, Academic Press, New York, 1979.
4. E. Snitzer: "Cylindrical Dielectric Waveguide Modes," *JOSA*, **51**(5) May 1961.
5. E. Jahnke and P. Emde: *Table of Functions with Formulas and Curves*, Dover Publications, New York, 1945.
6. T. Kimura, M. Saruwatari, J. Yamada, S. Uehura, and T. Miyashita: "Optical Fiber (800 Mbit/sec) Transmission Experiment at 1.05 μm," *Appl. Opt.*, **17**: 2420, Aug. 1, 1978.
7. D. E. Gray: *American Institute of Physics Handbook*, McGraw-Hill Book Co., New York, 1972.
8. D. N. Payne and W. A. Gambling: "Zero Material Dispersion Optical Fibers," *Electron. Lett.*, **11**: 176-178 (1975).
9. A. Kawana, M. Kawachi, and T. Miyashita: "Pulse Broadening in Long-Span Single Mode Fibers Around a Material-Dispersion Free Wavelength," *Opt. Lett.*, **2**(4), April 1978.
10. D. Gloge: "Dispersion in Weakly Guiding Fibers," *Appl. Opt.*, **10**(11), November 1971.
11. A. W. Snyder: "Asymptotic Expressions for Eigenfunctions and Eigenvalues of a Dielectric Optical Waveguide," *IEEE Trans. Microwave Theory Tech.*, **MTT-17**: 1130-1138, December 1969.
12. D. Gloge: "Weakly Guiding Fibers," *Appl. Opt.*, **10**: 2252-2258, October 1971.
13. D. Marcuse: *Theory of Dielectric Optical Waveguides*, Academic Press, New York, 1974.
14. M. Abromowitz and I. A. Stegun: "Handbook of Mathematical Functions with Formulas, Graphs and Mathematical Tables," *Natl. Bur. Stand. U.S. Appl. Math. Ser.*, **55** (1965).
15. D. Gloge: "Optical Power Flow in Multimode Fibers," *BSLTJ*, **51**(8), October 1972.

## PROBLEMS

- 5-1 Starting with Eq. (3-25) for  $H_r$  in cylindrical coordinates, derive Eqs. (5-20) and (5-26) for  $H_r$  in the core and cladding of a step-index fiber.
- 5-2 Calculate the pulse-delay distortion for a 1-km single-mode fused-silica step-index guide if  $\lambda_0 = 1.0 \mu\text{m}$ ,  $\Delta\lambda/\lambda = 0.12\%$ ,  $V = 1.5$ ,  $n_1 = 1.453$ ,  $n_2 = 1.450$ . Compare the pulse-delay distortion of the single-mode guide to the modal waveguide delay of a 1-km step-index multimode guide,  $V = 38$ ,  $n_1 = 1.453$ ,  $n_2 = 1.438$ .
- 5-3 Design a single-mode guide for operation at  $\lambda = 1.3 \mu\text{m}$  with a fused silica core ( $n_1 = 1.458$ ). Specify  $n_2$  and  $a$  for the guide. Will the guide still be single-mode if  $\lambda = 0.82 \mu\text{m}$ ? If not, how many modes will exist?

5-4 Calculate the  $V$  number and numerical aperture of a multimode guide if  $n_1 = 1.450$ ,  $\Delta = 1.3\%$ ,  $\lambda_0 = 0.82 \mu\text{m}$  and  $a = 25 \mu\text{m}$ . What happens to the number of modes in the guide if  $n_1$  increases? If  $n_1$  decreases? If  $\lambda_0$  increases? If  $\lambda_0$  decreases?

5-5 Obtain the characteristic equation for the step-index fiber equation (5-36) by expanding the determinant (5-35).

5-6 Starting with Eq. (5-36) derive the cutoff conditions for the  $\text{HE}_{1s}$  and  $\text{EH}_{1s}$  modes.

5-7 Identify which modes exist and specify the cutoff parameter ( $\kappa_c a$ ) for each mode in a step-index fiber with  $V = 5.5$ .

5-8 Calculate the material dispersion component of delay distortion for  $\lambda_0 = 0.8$ ,  $0.9$ ,  $1.3$ , and  $1.5 \mu\text{m}$  for a fused silica single-mode fiber. Assume in each case the source linewidth  $\Delta\lambda = 3 \text{ nm}$  and the guide length  $L = 1 \text{ km}$ .

5-9 Starting with Eqs. (5-81) and (5-82), derive Eq. (5-89), the characteristic equation for the LP modes. State the assumptions used in this analysis.

5-10 For a step-index fiber with  $V = 20$ ,  $\lambda = 0.82 \mu\text{m}$  and  $a = 25 \mu\text{m}$ , calculate the principal mode number  $M$ , the number of propagating modes, the semiangle of radiation  $\theta_0$ , and the difference in propagation direction of two neighboring mode groups  $\Delta\theta_0$ .

5-11 Calculate the percentage of power in the core and in the cladding for an LP<sub>11</sub> mode with  $\kappa_c a = 2.400$ .